Drug Screening Using Drug-Induced Haploinsufficiency in *Saccharomyces cerevisiae*

（出芽酵母のハプロ不全性に基づくドラッグスクリーニング）

２００８年

修士論文

東京大学大学院新領域創成科学研究科

先端生命科学専攻

生命応答システム分野

学籍番号：66520

小泉　貴弘

指導教員　大矢　禎一

Drug screening using drug-induced haploinsufficiency in Saccharomyces cerevisiae

Takahiro Koizumi

Department of Integrated Biosciences
Graduate School of Frontier Sciences
The University of Tokyo

2008

Master Thesis

出芽酵母のハプロ不全性に基づくドラッグスクリーニング

2008年3月修了
先端生命科学専攻　生命応答システム分野
学生証番号 ６６５２０　氏名　小泉　貴弘
指導教員　大矢　禎一 教授

キーワード：cerevisiae, haploinsufficiency, drug, yeast

天然化合物は化学構造や生物活性が多様であるため、創薬資源として高い可能性を秘めている。実際に、市場に出回っている薬剤のほとんどは天然物か天然物をモデルとして化学合成された誘導体である。しかし、現在使用されている薬剤は生体内の作用標的やその作用機構が未知のまま使用されているものも多く、細胞内における薬剤の標的タンパク質を同定することは、その薬理作用の分子機構を解明する上で極めて重要である。現在のところ、薬剤標的タンパク質の体系的な同定方法は確立していないが、近年、出芽酵母を用いたケミカルゲノミクス的な手法で薬剤標的の同定や作用機構の解明が試みられている。例えば、薬剤標的タンパク質をコードする遺伝子のコピー数が減少している二倍体ヘテロ型遺伝子破壊株がその薬剤に対して高い感受性を示すという、薬剤誘導型ハプロ不全性(drug-induced haploinsufficiency)を用いて、薬剤処理の有無で生じる増殖の差を多数の遺伝子破壊株を用いてプロファイリングすることで、その薬剤の標的タンパク質を同定する方法(HIP assay)が提案された(Lim *et al.*, 2003; Giaever *et al.*, 1999)。

そこで、本研究では、薬剤誘導型ハプロ不全性 を天然化合物スクリーニングに取り入れ、天然化合物のスクリーニングとその標的タンパク質の同定を同時並行的に行うことにより、有用化合物とその標的タンパク質を取得することを目的とした。

【結果と考察】

ストラテジー

薬剤誘導型ハプロ不全性 を用いた天然化合物スクリーニングのストラテジーを図 1 に示す。このスクリーニング系の利点として以下の 4 点が挙げられる。(1)標的遺伝子をあらかじめ選択することで、得たい作用活性を持つ化合物を効率よくスクリーニングできることが期待される。(2) 二倍体ヘテロ型遺伝子破壊株を用いて増殖を指標にスクリーニングを行うことにより、必須遺伝子を対象 とすることが可能になる。(3)薬剤に対する前提知識がなくてもアッセイを行うことが可能である。(4)96 well microplate 上などでスループットの高いアッセイが可能である。

図 1. 薬剤誘導型ハプロ不全性 スクリーニングのストラテジー(3rd STEP～4th STEP)

天然化合物スクリーニング

日本の土壌に生息しているカビや放線菌の細胞抽出物 4960 サンプルを対象に、天然化合物スクリーニングを行った(表 1)。まず、サンプル濃度 5%(v/v)で野生型株に対する細胞毒性を確認した(1st STEP)。次に、野生型株に対する最小増殖阻害濃度を決定した(2nd STEP)。決定した作用濃度を基にして、94 の二倍体ヘテロ型必須遺伝子破壊株を対象に薬剤誘導型ハプロ不全性スクリーニングを行った(3rd STEP)。そして、最後に破壊株特異的な増殖阻害を示したサンプルから化合物の単離・同定を行った(4th STEP: 産総研・新家研との共同研究)。その結果、reticulol、neocarazostatin A、neocarazostatin B、tensidol B、cycloheximide、barceloneic acid、3874H1 の 7 種の化合物が 94 株の二倍体ヘテロ型必須遺伝子破壊株のいずれかに対し特異的に増殖を阻害する、すなわち薬剤誘導型ハプロ不全性 を示す化合物として同定された。

表 1. スクリーニングの進捗状況

STEP	陽性サンプル / 試験サンプル
1	482 / 4960
2	280 / 482
3	15 / 280
4	7 / 15

neocarazostatin A の標的遺伝子産物の探索

天然化合物スクリーニングで同定された化合物のうち、抗菌活性や細胞毒性の報告がなく、新規の作用機序をもつと考えられる neocarazostatin A に注目して薬剤標的の探索を行った。まず、標的遺伝子の探索対象を 1112 ある全ての必須遺伝子 に拡大し、薬剤誘導型ハプロ不全性 スクリーニングを行った(図 2)。その結果、*sec7/SEC7*, *spc98/SPC98*, *gsp1/GSP1*, *yjr023c/YJR023c* の 4 株が、neocarazostatin A に対して高い感受性を示すことがわかった。この中で、Ran-transport protein をコードする *GSP1* については、Gsp1p の機能が失われると核移行シグナル(NLS)を持つタンパク質の核への局在が阻害されることが報告されている(Schlenstedt *et al.*, 1995)。そこで、野生型株および *gsp1/GSP1* 株を neocarazostatin A 処理した時の NLS-GFP の局在を観察した。その結果、neocarazostatin A 処理細胞においても NLS-GFP の核への局在が観察され、neocarazostatin A は Gsp1p の機能を阻害していないことがわかった(図 3)。このことから、neocarazostatin A の標的遺伝子は *GSP1* ではなく、他の候補遺伝子のいずれかであることが示唆された。

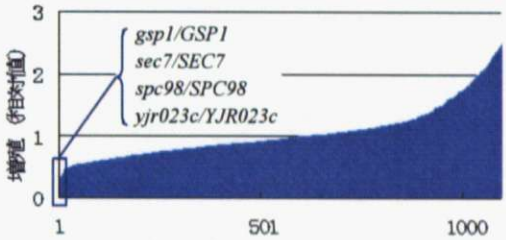

図 2. 必須遺伝子破壊株 1112 株に対する薬剤誘導型ハプロ不全性 の確認

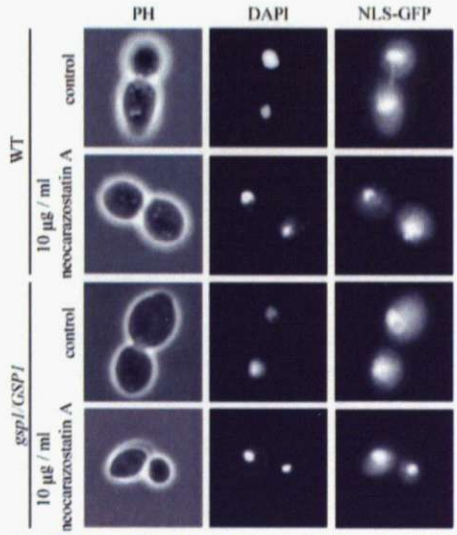

図 3. neocarazostatin A 処理した細胞における NLS -GFP の核局在の確認

【まとめ】

薬剤誘導型ハプロ不全性 を用いた天然化合物のスクリーニングを試み、neocarazostatin A を含む 7 個の化合物を得た。neocarazostatin A について、標的の同定を試み、候補を 3 つまで絞り込んだ。今後は、neocarazostatin A および他の薬剤の標的遺伝子の同定を完了させることで、このスクリーニングの有効性を示せると考えられる。

Table of Contents

List of Figures

List of Tables

Acknowledgements

I wish to express my deepest gratitude to an outstanding and experienced Geneticist, Prof. Yoshikazu Ohya for his supervision and advice throughout this study.

I also wish to express my gratitude to Associate Prof. Kintake Sonoike for his insightful suggestions and patient encouragement throughout this study.

I thank Dr. Satoru Nogami for his helpful advice, discussion and encouragement.

I would also like to express my sincere gratitude to Machika Watanabe, Takahiro Negishi and Shinsuke Ohnuki for great help.

I would like to thank Miki Maeda for her technical support.

I would like to thank Dr. Naoyuki Hayashi providing *gsp1* ts mutants.

I would like to thank Dr. Kazuo Shinya and Dr. Motoki Takagi providing screening samples and collaborating for isolation and identification of compounds.

I also thank all members of the Laboratory of Signal Transduction, Department of Integrated Biosciences, Graduate School of Frontier Sciences, the University of Tokyo, for their encouragement.

I am grateful to Kazuhiro Hananoi and Mio Tamori for their mental supporting.

Last but not least, I also thank my family for mental and financial support.

Abbreviations

AIST : National Institute of Advanced Industrial Science and Technology

DAPI : 4',6-diamidino-2-phenylindole

MIC : minimal inhibitory concentration

NEDO : New Energy and Industrial Technology Development Organization

NLS : nuclear localization signal

OMIM : Online Mendelian Inheritance in Man

PCR : polymerase chain reaction

SGD : *Saccharomyces* Genome Database

SGDP : *Saccharomyces* Genome Database Project

(http://www-sequence.stanford.edu/group/yeast_deletion_project/deletions3.html)

ts mutant: temperature-sensitive mutant

WT : wild type

Summary

Natural products have historically been a rich source of lead molecules in drug discovery. Actually, many of marketed compounds are the natural product origin. However, many drugs currently in use were discovered without knowledge of their underlying molecular mechanisms. Therefore, one of the major challenges in drug discovery is to identify the protein and cellular pathways affected by a drug. To identify the target of drugs, the budding yeast *Saccharomyces cerevisiae* is a valuable model organism because it is genetically tractable and it shares functional homologs with humans. In yeast, one of the powerful approaches to identify drug targets and to presume these pathways is drug-induced haploinsufficiency. Using drug-induced haploinsufficiency, it is possible to infer mechanism of action by comparing the changes elicited by drug treatment among heterozygous mutants. In this study, I constructed a novel screening system that uses drug-induced haploinsufficiency. To obtain useful natural compounds and their target candidates, I performed drug-induced haploinsufficiency screening with 94 heterozygous essential gene deletion strains. Among 4960 natural extracts samples tested, 7 natural compounds that induced haploinsufficiency for specific mutants were identified. One of these compounds, neocarazostatin was newly found to have antifungal activity or cytotoxicity towards *S. cerevisiae* and its target candidates were predicted by drug-induced haploinsufficiency. Consequently, to identify the target of neocarazostatin A, I performed large-scale mutant screening and narrowed down its candidates. To obtain many mutants that show

drug-induced haploinsufficiency, 1112 heterozygous essential gene deletion strains were used and drug-induced haploinsufficiency screening was performed. Intense growth inhibition activity was observed in 4 mutants: *yjr023c/YJR023C*, *sec7/SEC7*, *spc/SPC98* and *gsp1/GSP1*. A mutation in *GSP1* causes inhibition of protein nuclear translocation (Schlenstedt *et al.*, 1995). To examine whether Gsp1p was the target of neocarazostatin A, nuclear translocation of *gsp1/GSP1* in the presence of neocarazostatin A was observed. As a result, nuclear translocation was observed both in *gsp1/GSP1* and WT treated with neocarazostatin A at MIC. This result suggests that neocarazostatin A does not inhibit the function of Gsp1p at MIC. Further experiments will determine the targets of compounds isolated in this study, and the screening method will be useful to potentially isolate and identify novel useful compounds and their targets using *S. cerevisiae*.

Introduction

Natural compounds offer unmatched chemical diversity with structural and biological potency and occupy a complementary region of chemical space compared with synthetic compounds. Therefore, natural compounds have higher potential as drug discovery resource. In the areas of cancer and infectious diseases, 60% and 75% of new drugs, respectively, developed between 1981 to 2002, originated from natural sources. Between 2001 to 2005, 23 new drugs derived from natural products were introduced for the treatment of disorders such as bacterial and fungal infections, cancer, diabetes, dyslipidemia, atopic dermatitis, Alzheimer's disease and genetic diseases such as tyrosinaemia and Gaucher disease (Lam *et al.*, 2007). However, many drugs currently in use were discovered without knowledge of their underlying molecular mechanisms. On a molecular level, small molecular compounds act on cellular proteins as nutrients, toxins and therapeutic agents. Knowledge of the spectrum of cellular proteins targeted by compounds would greatly facilitate drug development. For example, identifying the protein targets of therapeutic natural compounds can reveal sources of pharmacologically undesired side effects in addition to the mechanisms for unwanted toxicities. Moreover, understanding the molecular mechanisms for therapeutic natural compounds is also critical because it allows researchers to develop second-generation compounds with improved pharmacological properties (Armour *et al.*, 2005). Therefore, the identification of the target of a compound and the elucidation of action mechanism are major problems in drug discovery.

The budding yeast *Saccharomyces cerevisiae* has contributed much to our knowledge of eukaryotic cell regulation. By using phenotypic readouts such as cell viability and morphological alterations, the genetic interaction between two genes can be examined by mutations in both genes, which has been a powerful tool in yeast to discover and characterize biological pathways. In fact, cellular target of rapamycin, an immunosuppressant used as an antirejection drug in matter of transplants, was first discovered in yeast and subsequently verified in humans (Heitman *et al.*, 1991; Huang *et al.*, 2004). In addition, Chan *et al.* screened 2226 non-essential deletion mutants with the immunosuppressant drug rapamycin. They identified 106 mutants displaying increased rapamycin sensitivity, only some of which were previously known to be more sensitive to rapamycin, thus considerably extending knowledge of the cellular functions of the 'Target of Rapamycin' pathway (Chan *et al.*, 2000). In 1996, the decoding of *S. cerevisiae* genome sequence was completed (Goffeau *et al.*, 1996), and it was demonstrated that the budding yeast genome is composed of about 1200 essential genes and about 5000 non-essential genes. The availability of complete genome sequences has yielded the ability to perform high-throughput, genome-wide screens of gene function. In addition, *S. cerevisiae* has been proposed as a tool for identifying human drug targets because over 40% of yeast proteins share some conserved sequence with at least one known or predicted human protein, including several hundred genes implicated in human diseases (Parsons *et al.*, 2003; Hughes, 2002). Recent technological advances in yeast genomics, including gene expression profiling, gene overexpression and haploinsufficiency, show promise as tools to study proteins and pathways affected by

drugs at a genome-wide level (Sturgeon *et al.*, 2006). Drug-induced haploinsufficiency is defined to occur when lowering the dosage of a single gene from two copies to one copy in diploid cells results in a heterozygote that displays increased drug sensitivity compared with WT (Giaever *et al.*, 1999; Baetz *et al.*, 2004). It is possible to infer mechanism of action from comparing the changes in gene expression elicited by drug treatment. For example, the novel target of 5-Fluorouracil (5-FU) was discovered using haploinsufficiency. 5-FU is an antimetabolite used to treat a wide variety of cancers, and it inhibits thymidylate synthase *CDC21* and causes misincorporation of fluoronucleotides into RNA and DNA. Treatment of the heterozygous deletion pool with 5-FU revealed drug-induced haploinsufficiency for eight genes that play roles in ribosome biogenesis in addition to the previously reported target *CDC21.* Four of 8 genes encode components of the exosome. The other 4 genes play roles in rRNA processing, ribosome production and other nucleolar components. As a result of further analysis, specific molecular mechanism by which 5-FU inhibits cell growth through perturbation of rRNA processing by the exosome complex was revealed (Lum *et al.*, 2004). A follow-up study indicated that 5-FU indeed inhibits an exosome-dependent surveillance pathway that degrades polyadenylated precursor ribosomal RNAs (Fang *et al.*, 2004). By providing a molecular explanation for the previously observed effects of 5-FU on RNA metabolism, these studies uncovered an important aspect of the mechanism of action of 5-FU.

Specific small compound-protein interactions are often identified genetically followed by *in vitro* characterization. However, such chemical genomic methods are

effective only for target identification of known compounds whereas are ineffective for natural compound screening handling a large number of samples. In this study, I thought that it is possible to apply drug-induced haploinsufficiency to drug screening. I constructed new screening system using drug-induced haploinsufficiency, and performed the screening of natural compounds with selected deletion mutants of genes, of which homologs are involved in human diseases and of genes participating in basic cellular functions. To obtain the sample and its specific targets, I have performed drug-induced haploinsufficiency screening with 94 heterozygous essential gene deletion mutants. As a result, 7 compounds which showed drug-induced haploinsufficiency to one or more of the mutants were obtained. Neocarazostatin A was one of the compounds. To obtain further information on potential targets of neocarazostatin A, I performed drug-induced haploinsufficiency screening with 1120 essential deletion strains. As a result, 4 mutants were obtained. Target validation of neocarazostatin A was performed.

Results

Premise for Drug-Induced Haploinsufficiency Strategy

To screen the natural compounds having a key bioactivity from large-scale samples, I employed the haploinsufficiency screening as a screening method enabling us to cover the essential genes (Figure 1a-1). Although conventional methods of the haploinsufficiency screening is enough to high-throughput mutant screening because of the use of DNA microarray, the method is too expensive for large-scale sample screening (Figure 1a-2). Then, I employed the liquid culture method instead of DNA microarray to assess the drug-induced haploinsufficiency (Figure 1b). Although a number of mutants we can treat by the liquid culture assay is fewer than that of DNA microarray, the liquid culture assay is suitable to the large-scale drug screening in this study because we can find the compounds which relate to the intended gene functions without the knowledge of the compounds by defining the mutants. Thus, high-throughput and high-cost performance large-scale drug screening in high-efficiency became feasible with four advantages as follows: 1) the compounds are efficiently screened by defining mutants, 2) the cost performance is higher than the DNA microarray by using the liquid culture assay, 3) the researchers need not to have the detailed knowledge of the compounds, 4) the 96-well microplate as a high-throughput experimental equipment is applicable to this approach. Therefore, I defined the 94 mutants from 1112 heterozygous essential gene deletion strains, and most of these mutants are known as disease-related human gene homologs (Table 1). The

experiment scheme having these advantages was shown in Figure2.

Preliminary Experiments to Examine Inoculation Method and to Confirm Culture Condition

To screen the samples by the strategy shown in Figure 2, culture in a 96-well microplate needed to be in an appropriate range (0.1-0.7) for absorption spectrometer used in this study when measuring OD 600. Then, I tested two inoculation methods using WT yeast strains to acquire uniformly controlled cell cultures. The two inoculation methods are as follows. 1) WT cells were inoculated from a dish of overnight culture to a 96-well microplate containing 100 μl of YPD medium using a set of 96 pins (pin method) and 2) overnight culture was diluted 100-fold in YPD liquid medium, and 100 μl was dispensed to 96-well microplate (pipette method). Distributions of OD 600 after 6 hours of culturing using each inoculation method is shown in Figure 3a. The pipette method was more uniformly controllable than the pin method because distribution range of the pipette method was smaller (Figure 3a), suggesting that the pipette method is suitable to this study. Therefore, I employed the pipette method to drug screening of this study.

Next, to optimize dilution procedure of the pipette method, I compared effects of three dilution procedures on uniformity of OD 600. Three procedures to dilute each culture solution to 100-fold were as follows, 1) diluting to 100-fold by one-step (one-step dilution), 2) diluting to 10-fold again after a 10-fold dilution and 3) diluting to 50-fold after a 2-fold dilution. Distributions of OD 600 after 6 hours of culturing using

each dilution procedure is shown in Figure 3b. The one-step dilution procedure was the most uniformly controllable procedure among the three because distribution range of the procedure was the smallest (Figure 3b), suggesting that the one-step dilution procedure is suitable to this study. Therefore, I employed the one-step dilution procedure to the pipette method (one-step pipette method) in this study.

To decide culture time for the drug screening, I compared dispersions of OD 600 among every two hours from 14 hours to 20 hours of culture time. The pre-culture of WT was prepared with 96-well microplate instead of dishes and inoculated to another 96-well microplate with one-step pipette method. The distribution of OD 600 after incubation for 6 hours was shown in Figure 3c-1. The dispersion of Figure 3c-1 was 0.111 ± 0.003 (mean ± SD), suggesting that the one-step pipette method resulted in enough uniformity of WT cell culture for the drug screening in this study. Subsequently, 15 μl of 200-fold diluted pre-culture was inoculated to 85 μl YPD prepared in 96-well microplate and OD 600 was measured at each time point. Experiments were triplicated and the mean values of OD 600 in each 96-well microplate were shown in Figure 3c-2. OD 600 from 16 hours to 20 hours were in the appropriate range for absorption spectrometer and mean values of coefficient value (CV) of each SD were 0.128 ± 0.002, 0.153 ± 0.003 and 0.131 ± 0.012 (mean ± SD), respectively, suggesting that incubating for 16 hours resulted in the most uniform WT cell culture condition.

Lastly, preparing the pre-culture of 94 mutants which were used in the drug-induced haploinsufficiency screening, OD 600 of these mutants incubated for 16 hours are shown in Figure 3d. The mean value of OD 600 was 0.106 ± 0.003 (mean ±

SD, n=94) in Figure 3d, suggesting that the incubation for 16 hours after the preparation of pre-culture with the one-step pipette method give us the condition of uniform culturing within the appropriate range for the absorption spectrometer for the drug screening in this study.

Screening of Natural Compounds

Screening of natural compounds inducing the growth inhibition to WT (1st STEP)

To find samples containing bioactive compounds, I tested 4960 samples for the growth inhibition to WT by adding 5% (v/v) of samples. The growth inhibition was assessed by my eyes instead of OD 600 values of the culture. Samples which showed growth inhibition activity to WT were 482 samples among 4960 samples (Table 4).

Estimation of the minimal inhibitory concentrations (MIC) to WT (2nd STEP)

To determine the MIC which is minimal concentrations inducing growth inhibition to WT, I tested for the growth inhibition assessed by my eyes to WT by adding samples at eight different concentrations which were eight serial dilution of 2-fold from 5%. At the same time reproduction of the 1st STEP was confirmed at the 5% (v/v) of samples. Among 482 samples, reproducibility of 1st STEP to 280 samples was confirmed (Table 4), and MIC for the samples was determined.

Drug-induced haploinsufficiency screening (3rd STEP)

To screen the sample containing compounds which cause drug-induced haploinsufficiency, I tested for the growth inhibition of the 94 mutants by adding samples at half of MIC determined in 2nd STEP. Assessed by my eyes, 15 of the 280

samples caused the drug-induced haploinsufficiency (Table 4 and 5). Here, for an example as a part of the results of drug-induced haploinsufficiency screening, I pointed 4 of 15 samples. For the 4 samples selected, similar assay was performed and OD 600 values of mutants grown in the presence of the sample were measured and compared with control value of OD 600 (Figure 4). In Figure 4, the mutants having less than 0.4 of the relative ratio (drug OD 600 / control OD 600) were judged to be caused the drug-induced haploinsufficiency by the sample. Specific growth inhibition was presented again with 3 samples: NT40Q (for *sec7/SEC7*), NU15Q (for *iog1/IOG1*) and FD40R (for *spt14/SPT14*) (Figure4, Table 5). NT39K induced growth inhibition for 9 strains containing *cks1/CKS1* and *arp2/ARP2* (Figure 4, Table 5).

Isolation and identification of compounds (4^{th} STEP)

Isolation and structure analysis of compounds was performed by Dr. K. Shinya (AIST) and collaboration with M. Watanabe. As a result, 7 known bioactive compounds were isolated and identified from 6 samples among 15 samples. Structures of these compounds were shown in Figure 5.

Large-Scale Mutant Screening towards Identification of the Target Gene of Neocarazostatin A

Because the cytotoxicity of neocarazostatin has never been reported, I focused on NT40Q containing neocarazostain A/B as novel cytotoxic compounds. To identify target genes of neocarazostatin, I screened the 1112 of heterozygous essential gene deletion mutants by the drug-induced haploinsufficiency screening. Using NT40Q, I

obtained relative ratio of 1112 mutants by the method of 3rd STEP of Figure 2 (Figure 6a). Twenty one of 1112 mutants had less than 0.5 of relative ratio and 3 of the 21 mutants had remarkably low values (Figure 6b). Two of the 3 mutants (*yjr023c/YJR023C* and *spc98/SPC98*) were novel sensitive mutants and the other (*sec7/SEC7*) was the mutant strain used in the previous step of drug screening (*sec7/SEC7* (94)). Although *sec7/SEC7* (94) was successfully screened again, another mutant strain of *sec7/SEC7* which was in the 1112 mutants (*sec7/SEC7* (1112)) was not screened as sensitive.

Because the 1112 mutants were divided to 13 microplates and independently screened by each microplate, I screened 10 mutants having less than 0.4 relative ratios on a single microplate, excluding differences between microplates (Figure 6c). In addition, to confirm the result of Figure 6c, I conducted the same assay using purified neocarazostatin A in the same way (Figure 6d). From the screening results of Figure 6c and d, 4 mutant strains (*yjr023c/YJR023C*, *sec7/SEC7* (94), *spc98/SPC98* and *gsp1/GSP1*) were firmly identified as mutants that the drug-induced haploinsufficiency was observed by neocarazostatin A, therefore these deleted genes are regarded as candidates of targets of neocarazostatin A.

Confirmation of Deletion Genotype of Neocarazostatin Sensitive Mutants

To confirm that the gene deletion is one of the causes to result in high sensitivity, I verified the replacement of the yeast genes by the kanamycin resistance gene cassette by PCR using genomic DNA as a template. With a protocol of

Saccharomyces Genome Deletion Project (SGDP), correct deletion of all of 4 genes was confirmed. As for *sec7/SEC7* (94), I additionally confirmed two other strains: 1) *sec7/SEC* (tube), the parent strain of the *sec7/SEC7* (94) and 2) *sec7/SEC7* (1112), the strain used in screening of 1112 mutants, and correct deletions in both of *sec7/SEC7* (tube) and *sec7/SEC7* (1112) were confirmed (Figure 7). Although the reasons of difference between phenotypes of *sec7/SEC7* (94) and *sec7/SEC7* (1112) strains are unknown, high sensitivity of 4 mutants were assumed to be caused by the gene deletion.

Next, to confirm the drug sensitivity of mutants, I tested for the concentration-dependence of drug sensitivity in the mutants. Excluding *spc98/SPC98*, 3 of the 4 mutants were sensitive in a concentration-dependent manner at higher or equal to 5 μg/ml of neocarazostatin A, and for *spc98/SPC98* was in a concentration-dependent manner at higher or equal to 8 μg/ml (Figure 8). All of the mutants were in a concentration-dependent manner at lower concentration than WT, indicating that these genes could be the target of neocarazostatin A.

Effects of Neocarazostatin A on the Function of Gsp1p

At the restrictive temperature, *gsp1* ts mutant (N43-6C *gsp1-479*) is known as nuclear transport defective (Schlenstedt *et al.*, 1995; Oki *et al.*, 1998). Therefore I suspected that *gsp1/GSP1* mutant treated with high-concentration of neocarazostatin A is defective in nuclear localization of nuclear localization signal (NLS) protein. Then, 4 mutants of N43-6C *GSP1*, N43-6C *gsp1-479*, BY4743 and *gsp1/GSP1* carrying *pADH-NLS-GAL4AD-EGFP* (NLS-EGFP), were constructed to visualize the subcellular

NLS localization.

Firstly, to confirm construction, I tested for NLS-EGFP translocation of N43-6C *gsp1-479* in restrictive temperature (Figure 9a). Nuclear translocation of NLS-EGFP was successfully inhibited at the restrictive temperature, therefore I compared accumulation transition of cells which are inhibited NLS-EGFP translocation between N43-6C *gsp1-479* at restrictive temperature and controls (Figure 9b). These results suggest that the constructions were correctly transformed.

Secondly, to test whether neocarazostatin A inhibits Gsp1p, I compared accumulation transition of cells which is inhibited NLS-EGFP translocation between *gsp1/GSP1* in 5 μg/ml of neocarazostatin A and controls (Figure 10). Nuclear translocation was observed in each mutant (Figure 10), suggesting that 5 μg/ml of neocarazostatin A did not inhibit nuclear translocating function of Gsp1p.

Lastly, to test whether neocarazostatin A inhibits Gsp1p, I compared in the same way at 10 μg/ml of neocarazostatin A (Figure 11). However, nuclear translocation was observed again in each mutant (Figure 11), suggesting that 10 μg/ml of neocarazostatin A did not inhibit nuclear translocating function of Gsp1p. These results suggest that the inhibition of nuclear translocation by neocarazostatin A is not observable at lower or equal to 10 μg/ml of neocarazostatin A.

Discussion

In this study, liquid culture assay was performed in parallel on 96-well microplate, and differences in drug sensitivity among mutants were used as an index to evaluate drug activity. Drug screening of the yeast which assumed the growth in the liquid medium an index is performed by Toussaint and the activity of the drug is evaluated by calculating lag time from growth curve of the yeast (Toussaint *et al.*, 2006). In this study, methodology of drug screening using *S. cerevisiae* culture in 96-well microplate was established and in addition, possibility of using drug-induced haploinsufficiency in diploid *S. cerevisiae* to determine the target of the active compound was explored. In combination, it provides us with a strong method in screening large number of compounds and heterozygous mutants of essential genes systematically using growth as an index to evaluate drug activity. As a result, successful manipulation of liquid culture that is advantageous in drug screening was demonstrated and candidates of targets of several active compounds have been implied.

Preliminary Experiments to Examine Inoculation Method and to Confirm Culture Condition

First, it was necessary to establish manipulation of yeast culture in 96-well microplate in order to ensure the sensitive screening procedure. Therefore, to treat yeast in 96-well microplate uniformly, reproducibly and in parallel, preliminary experiments of inoculation method and confirmation of culture condition were performed. To

determine suitable inoculation method, the precision of two inoculation methods (pin method and pipette method) were compared using WT strain. As a result, dispersion in growth or values of OD 600 of separately manipulated cultures of inoculation by pipette method was smaller than that of pin method. Although the throughput by pin method was higher than the throughput by pipette method, pipette method was adopted to give priority to precision of inoculation. Next, to examine the dilution method which confers the minimal dispersion in OD 600 values by pipette method, dilution methods were optimized. As a result, it was determined that inoculation performed by one-step of 100-fold dilution minimized the dispersion. It was suggested that dispersion of the inoculation was minimized by reducing the frequency of dilution. Dispersion in OD 600 values of otherwise equally treated samples are thought to originate in the marginal error in the use of pipette. Whether human or systematic error occurred in pipetting, it is concluded that less frequent dilution by pipetting is more suited in this assay. It was confirmed that uniformity of growth on 96-well microplate by pipette inoculation method can be achieved by the actual condition of screening described in Materials and Methods. As in Figure 3c-1, OD 600 of about 90% WT cells showed around 0.125 and the dispersion of Figure 3c-1 was 0.111 ± 0.003 (mean ± SD), suggesting that the one-step pipette method resulted in enough uniformity of WT cell culture for the drug screening in this study. Subsequently, 15 μl of 200-fold diluted pre-culture was inoculated to 85 μl YPD prepared in 96-well microplate and measured OD 600 in each time point. Experiments were triplicated and the mean values of OD 600 in each 96-well microplate were shown in Figure 3c-2. OD 600 from 16 hours to 20 hours were

in range (0.1-0.7) of the absorption spectrometer and mean values of coefficient value (CV) of each SD were 0.128 ± 0.002, 0.153 ± 0.003 and 0.131 ± 0.012 (mean ± SD), respectively, suggesting that incubating for 16 hours resulted in the most uniform WT cell culture condition. Therefore, it was considered that it is possible to treat culture uniformly in actual condition of screening, which allows efficient systematic screening using 96-well microplate. However, the uniformity of the cultures was expected to be somewhat problematic when dealing with 94 heterozygous essential gene deletion strains (94 mutants) as in the 3rd step of the screening. To check uniformity of 94 mutants, which differed in doubling time, cultured in 96-well microplate (i.e. each individual well containing different mutant), 94 mutants were cultured in an actual condition of pre-culture in screening. As a result, OD 600 of all 94 mutant cells showed around 0.1 after 16 hours of incubation, which is in the appropriate range for the absorption spectrometer used. It was understood that 94 mutant cells were approximately treated uniformly in parallel. It is important to establish this methodology since the inhibition of growth in each mutant has to be detected through the absorption spectrometer and it is optimal to treat the cells when they are in logarithmic growth phase. In addition, because the dispersion of the triplicate result was small, reproducibility of the assay could be expected.

Screening of Natural Compounds

To screen compounds that induce growth inhibition in WT at 5%, growth inhibition test to WT was performed (1st STEP). As a result, there were 482 samples

which showed growth inhibition activity to WT among 4960 samples. It was understood that about 10% of the screening samples showed growth inhibition activity for WT at 5%. This validates the already known fact that natural compounds are ample reservoir of seed compounds for drug development. To determine the minimal concentrations that induce inhibition in WT, MIC of samples were estimated with 96-well microplates (2^{nd} STEP). As a result, reproducibility of 1^{st} STEP to 280 samples was confirmed among 482 samples, and MIC for the 280 samples were determined. Poor reproducibility may be a result of degradation of active compounds since some of the active molecules may be unstable. To screen the sample which shows drug-induced haploinsufficiency to the 94 mutants selected, drug-induced haploinsufficiency screening was performed (3^{rd} STEP). Fifteen samples resulted in drug-induced haploinsufficiency among 280 samples. However, it became a matter that reproducibility was poor. It was thought that since the sensitivity of the liquid assay was high, slight errors occurred in manipulation in every step of the assay influenced the result. In order to avoid the poor reproducibility, it is necessary to have more stringent cut-off values for drug-induced haploinsufficiency, which would reduce the number of false-positives in the screening. Isolation and structure analysis of compounds was performed by Dr. K. Shinya (AIST) and collaboration with M. Watanabe (4^{th} STEP). As a result, 7 known bioactive compounds were identified among 15 samples. One of the identified active compounds was neocarazostatin A/B. Neocarazostatin A/B are known to function in lipid antioxidation activity (Dr. K. Shinya, unpublished). The antibacterial activity and cytotoxicity are not known (Kato *et al.*, 1991; Czerwonka *et al.*, 2006). Tensidol B was also identified as the

active compound in the screen. It is known to potentiate miconazole activity against *Candida albicans.* Tensidols also showed moderate antimicrobial activity only against *Pyricularia oryzae.* (Fukuda *et al.*, 2006). Barceloneic acid was identified and it is known as inhibitor of farnesyl-protein transferase (FPTase) (Jayasuriya *et al.*, 1995; Overy *et al.*, 2005). Another active compound was reticulol. Reticulol is known to have antimycotic action for A427 (human lung tumor cell line) and B16F10 (mouse melanoma cell line) and it is reported that it inhibits mouse melanoma metastasis to lung presumably by inhibiting topoisomerase I of the melanoma cells (Lim *et al.*, 2003). The other was cycloheximide, which is a commonly used inhibitor of protein synthesis and lastly, 3874 H1 was identified which is a potent antifungal compound with a broad spectrum of activity, encompassing dermatophytes, yeasts and filamentous fungi (Vertesy *et al.*, 1998). In this screening method, both known and novel compounds were identified, which shows the credibility and novelty of the assay system. For the compounds of which cytotoxicity is not known, such as neocarazostatin A/B and reticulol, it is interesting to farther identify the targets or function of the compounds in the cell, possibly by the use of *S. cerevisiae* as model organism.

Large-Scale Mutant Screening towards Identification of the Target Gene of Neocarazostatin A

In order to obtain mutants which show drug-induced haploinsufficiency, 1112 heterozygous essential gene deletion strains were used and drug-induced haploinsufficiency screening was performed in YPD medium containing 0.625 % of

NT40Q (sample which neocarazostatin A/B was identified). As a result, intense growth inhibition activity was observed in 4 mutants: *yjr023c/YJR023C*, *sec7/SEC7*, *spc/SPC98* and *gsp1/GSP1*. Furthermore, to establish the same growth inhibition activity can be observed using purified neocarazostatin A, drug-induced haploinsufficiency screening was performed with 5 μg/ml of neocarazostatin A (half of MIC). As a result, the intense growth inhibition activity was observed in the 4 mutants, which are the same mutants as when NT40Q was used. It was implied that the target of neocarazostatin A is the product of one of the 4 genes. Although a growth inhibition activity was confirmed in *sec7/SEC7* (94) which is derived from 94 mutants used in the 3rd Step of screening, the growth inhibition activity was not confirmed in *sec7/SEC7* (1112) which was derived from the collection of 1112 essential gene heterozygous deletion strains. It was suggested that some kind of mutation entered to *sec7/SEC7* in either of the strains used and farther investigation is necessary. Even though the haploinsufficiency of *sec7/SEC7* can be disputed, it is clearly shown that the other heterozygous deletion strains such as *yjr023c/YJR023C*, *spc/SPC98* and *gsp1/GSP1* showed drug-induced haploinsufficiency. This result is expected to lead us to the potential target of neocarazostatin A and to the elucidation of its cytotoxicity.

Confirmation of Deletion Genotype of Neocarazostatin Sensitive Mutants

To ensure the gene deletions of mutants which showed sensitivity to neocarazostatin A, confirmation of deletions were established by PCR. Because growth inhibition activity of neocarazostatin A for *sec7/SEC7* was not observed in the strain

derived from the 1112 deletion collection, *sec7/SEC7* of 3 different stocks available in the laboratory were tested and confirmed to possess the right deletion. It was also confirmed that genes of heterozygous mutants for the three other mutants tested were deleted correctly. From this result, it was suggested that the deletion of *SEC7* may not be the cause to increase sensitivity to neocarazostatin A. Therefore, target validation of neocarazostatin A for *sec7/SEC7* was withheld. In addition, it was suggested that the investigation of *YJR023C* is difficult as the function of the gene is not known and there were little hereditary information. The candidate strains for which target validation of neocarazostatin A is performed were narrowed down to two mutants, *spc98/SPC98* and *gsp1/GSP1*. Assuming neocarazostatin A is inducing haploinsufficiency, the growth inhibition is expected to be in a concentration-dependent manner. To test this theory, growth inhibition of neocarazostatin A was performed at several concentrations using neocarazostatin A sensitive mutants. As a result, neocarazostatin A acted on concentration-dependent manner to all 4 mutants. *spc98/SPC98* had higher inhibitory concentration of neocarazostatin A in comparison with other mutants. It was suggested that the gene products of other mutants had higher possibility than Spc98p as the target of neocarazostatin. Therefore, this lead me to validate if neocarazostatin A targets Gsp1p.

Effects of Neocarazostatin A on the Function of Gsp1p

As discussed above, it seemed reasonable to test the effect of neocarazostatin A on Gsp1p. A mutation in *GSP1* causes inhibition of protein nuclear translocation

(Schlenstedt *et al.*, 1995). To examine that Gsp1p was the target of neocarazostatin A, nuclear translocation of *gsp1/GSP1* in the presence of neocarazostatin A was observed along with its WT control. As a result, nuclear translocation was observed both in *gsp1/GSP1* and WT at MIC of neocarazostatin A. This result indicates that neocarazostatin A does not inhibit the function of Gsp1p. However, MIC of 10 μg/ml may not have been sufficient to inhibit the translocation of NLS-EGFP used in the study and it is possible that the higher concentration of neocarazostatin A treatment may help visualize the mislocalization of NLS-EGFP through fluorescent microscopy.

For another perspective in elucidating the target of neocarazostatin, Spc98p can be investigated. Spc98p is known to function in formation of spindle microtubule by interacting with the major spindle pole body component, Spc110p (Nguyen *et al.*, 1998). When Spc98p is inhibited, the interaction between Tub4p and Spc110p is expected to be lost and the abnormal localization of nuclear microtubules is expected. This phenotype can be an indicator of neocarazostatin A targeting Spc98p. As a conclusion, among 4960 natural extracts samples tested, 7 natural compounds were identified through the screen developed to use liquid handling with 96-well microplate, and the targets of the compounds were screened simultaneously. Among the 7 compounds identified, neocarazostatin was newly found to have antifungal activity or cytotoxicity towards *S. cerevisiae* and its target is predicted by drug-induced haploinsufficiency. Further experiments will determine the targets of compounds isolated in this study, and the screening method will be useful to potentially isolate and identify novel compounds and

their targets using *S. cerevisiae*.

Materials and Methods

Yeast Strains, Media and Growth Conditions

A heterozygous essential strain collection created by the *Saccharomyces* Genome Deletion Project (SGDP) was purchased from Open Biosystems (Open Biosystems, USA). Ninety-four heterozygous deletion strains used in drug-induced haploinsufficiency screening in this study were shown in Table 1. Strains used for validation of pharmacological action were shown in Table 2. N43-6C *GSP1* and N43-6C *gsp1-479* were provided by Dr. N. Hayashi (Kanazawa University, Hayashi *et al.*, 2007). *S. cerevisiae* was grown either in YPD or SD medium. YPD medium contained 1% (w/v) bacto yeast extract (BD Biosciences, USA), 2% (w/v) bacto polypeptone (BD Biosciences, USA) and 2% (w/v) dextrose. SD medium contained 0.67% (w/v) yeast nitrogen base w/o amino acids (BD Biosciences, USA) and 2% (w/v) dextrose. Amino acids required by the strain (adenine, uracil, L-tryptophan, L-histidine-HCl, L-leucine and L-lysine-HCl (WAKO, Japan)) were added. Cells were incubated in YPD or SD medium at 25 °C unless noted.

Strain Confirmation

Confirmation of the deletion strains was carried out as described in SGDP. For amplification of disruption construct by PCR, extracted genome of the deletion strain and *TaKaRa Ex Taq*^{tm} polymerase (TaKaRa Biochemicals, Japan) were used. Primers used in this assay were shown in Table 3.

Screening of Active Compounds and Purification of Compounds

All screening samples and neocarazostatin A were provided by Dr. K. Shinya (AIST). Screening samples were crude extract of metabolites produced by actinomycetes or fungi. Microbial metabolites were extracted with 67% acetone solution + 33% pure water for actinomycete samples or 80% acetone solution + 20% pure water for fungus samples. These crude extracts were defined as 100% sample, and the dilution of these samples were used in this study.

Screening of Natural Compounds

For all the liquid handling on 96-well microplate (Corning, USA) or 96-deep plates (Nunc, Denmark), multi-pipetter Impact 2 (MATRIX, USA) was used. OD 600 was measured by Plate Reader SPECTRAMAX 384 plus (Molecular Devices, USA).

Screening of samples that induce growth inhibition in WT at 5% (1st STEP)

Culture of logarithmically growing WT cells was diluted to 5 x 10^4 cells/ml. Diluted culture (15 μl) was dispensed to each well of 96-well microplate. YPD or SD medium (85 μl) which contained the screening sample at 5.9% was added to each well to produce the final sample concentration of 5.0% in 100 μl culture. After cultured at 25 °C for 24 hours, growth inhibition was checked by visual observation. The assay was carried out both in YPD and SD media and the medium which inhibitory activity happened in lower concentration was chosen and used in the farther steps in the screening unless noted.

Estimation of the minimal inhibitory concentrations (MIC) to WT (2nd STEP)

Eighty-five μl of two-fold serial dilution (containing screening sample of 8 serial dilutions from 5.9% to 0.046%) were longitudinally dispensed to 96-well microplate. Culture of logarithmically growing WT cells was diluted to 5 x 10^4 cells/ml. Fifteen μl of cell diluted culture was dispensed to 96-well microplate to produce cultures containing serially diluted samples in 100 μl culture. After cultured at 25 °C for 24 hours, growth inhibition was checked by visual observation.

Drug-induced haploinsufficiency screening (3rd STEP)

Ninety-four heterozygous mutants were cultured overnight at 25 °C in 100 μl of YPD medium in 96-well microplate and were diluted 100-fold in 96-deep plate. One hundred μl of the diluted cultures was dispensed to another 96-well microplate and cultured at 25 °C for 6 hours. The absorbance was measured to confirm that OD 600 was around 0.1. It was then diluted 200-fold and 15μl of the culture was dispensed to 96-well microplate. Furthermore, 85 μl of appropriate medium containing screening sample was dispensed to produce cultures containing half of MIC (%) of the samples in 100 μl culture. Culture was incubated at 25 °C for 28 hours, and OD 600 was measured every two hours from 14 hours to 28 hours. In addition, growth inhibition was checked by visual observation.

Isolation and identification of compounds (4th STEP)

Isolation of the active compounds was carried out by collaborating with Dr. K. Shinya (AIST) as one end of NEDO project. The extract samples showed growth inhibition was fractionated by medium-pressure liquid chromatography (MPLC, Purif

α2, MORITEX, Japan). The purification of the compound was advanced by chasing the fraction which showed growth inhibition activity. This bioassay was performed by M. Watanabe (Department of Integrated Biosciences, Graduate School of Frontier Sciences, Tokyo University). Purification and bioassay were repeated several times, and finally identification of compound was performed using HPLC-Mass Spectrometry-NMR (VARIAN, USA).

Growth Inhibition Analysis

The ratio of OD 600 of drug treated strain and OD 600 of drug untreated strain (control) was calculated. In the case of YPD medium, the OD 600 value which showed approximately 0.1-0.2 was used. In the case of SD medium, the OD600 value which showed approximately 0.08 was used. Then the value was standardized so that the WT strain acquired the value of 1. The value was used for evaluation of the growth inhibition activity. This value was shown as "sample plate OD / control plate OD" in Figure 4 and Figure 6. Mutants which become "relative ratio < 0.4" were judged as showing drug-induced haploinsufficiency.

Introduction of NLS-EGFP

Plasmid pAUR101-*pADH-NLS-GAL4AD-EGFP* (pYO2350) (derived from pAUR101 (TaKaRa, Japan)) was digested with *Stu*I to linearize the plasmid in *AUR1-C* region of the vector. Linearized pYO2350 was then introduced to the appropriate yeast strains by standard lithium acetate transformation method for recombination. The

selection of the transformants was carried out using 0.5 μg/ml aureobasidin A (TaKaRa, Japan) containing YPD plate. Stable transformant was acquired by re-selecting the transformants on 0.5 μg/ml aurerobasidin A containing YPD plate. Authenticity of the recombination was checked by fluorescent microscopy.

Fluorescence and Microscopy

Cells were centrifuged at 12,000 rpm and its pellet was mixed with mounting buffer containing 1 μg/ml 4'6-diamidino-2-phenylindole (DAPI, WAKO, Japan) for DNA staining. Yeast cells were observed using a AxioImager M1 (Carl Zeiss, Germany) and Plan Apochromat 100x objective. Images were captured using a cooled CCD camera CoolSNAPHQ (Roper Scientific Photometrics, USA) interfaced with AxioVision (Carl Zeiss, Germany).

References

Armour CD, Lum PY.

From drug to protein: using yeast genetics for high-throughput target discovery. *Curr Opin Chem Biol* 2005, **9**: 20-4.

Baetz K, McHardy L, Gable K, Tarling T, Reb_rioux D, Bryan J, Andersen RJ, Dunn T, Hieter P, Roberge M.

Yeast genome-wide drug-induced haploinsufficiency screen to determine drug mode of action. *Proc Natl Acad Sci USA* 2004, **101**: 4525-30.

Chan TF, Carvalho J, Riles L, Zheng XF.

A chemical genomics approach toward understanding the global functions of the target of rapamycin protein (TOR). *Proc Natl Acad Sci USA* 2000, **97**: 13227-32.

Czerwonka R, Reddy KR, Baum E, Knolker HJ.

First enantioselective total synthesis of neocarazostatin B, determination of its absolute configuration and transformation into carquinostatin A. *Chem Commun* 2006, **7**: 711-3.

Fang F, Hoskins J, Butler JS.

5-fluorouracil enhances exosome-dependent accumulation of polyadenylated rRNAs. *Mol Cell Biol* 2004, **24**: 10766-76.

Fukuda T, Hasegawa Y, Hagimori K, Yamaguchi Y, Masuma R, Tomoda H, Omura S. Tensidols, new potentiators of antifungal miconazole activity, produced by *Aspergillus niger* FKI-2342. *J Antibiot* 2006, **59**: 480-5.

Giaever G, Shoemaker DD, Jones TW, Liang H, Winzeler EA, Astromoff A, Davis RW. Genomic profiling of drug sensitivities via induced haploinsufficiency. *Nat Genet* 1999, **21**: 278-83.

Goffeau A, Barrell BG, Bussey H, Davis RW, Dujon B, Feldmann H, Galibert F, Hoheisel JD, Jacq C, Johnston M, Louis EJ, Mewes HW, Murakami Y, Philippsen P, Tettelin H, Oliver SG.
Life with 6000 genes. *Science* 1996, **274**: 546, 563-7.

Hayashi N, Murakami S, Tsurusaki S, Nagaura Z, Oki M, Nishitani H, Kobayashi M, Shimizu H, Yamamoto K, Nishimoto T.
Temperature-sensitive defects of the *GSP1*gene, yeast Ran homologue, activate the Tel1-dependent pathway. *Biochem Biophys Res Commun* 2007, **353**: 330-6.

Heitman J, Movva NR, Hall MN.
Targets for cell cycle arrest by the immunosuppressant rapamycin in yeast. *Science* 1991, **253**: 905-9.

Huang J, Zhu H, Haggarty SJ, Spring DR, Hwang H, Jin F, Snyder M, Schreiber SL.
Finding new components of the target of rapamycin (TOR) signaling network through chemical genetics and proteome chips. *Proc Natl Acad Sci USA* 2004, **101**: 16594-9.

Hughes TR.
Yeast and drug discovery. *Funct Integr Genomics* 2002, **2**: 199-211.

Jayasuriya H, Ball RG, Zink DL, Smith JL, Goetz MA, Jenkins RG, Nallin-Omstead M, Silverman KC, Bills GF, Lingham RB, *et al.*
Barceloneic acid A, a new farnesyl-protein transferase inhibitor from a Phoma species. *J Nat Prod* 1995, **58**: 986-91.

Kato S, Shindo K, Kataoka Y, Yamagishi Y, Mochizuki J.
Studies on free radical scavenging substances from microorganisms. II. Neocarazostatins A, B and C, novel free radical scavengers. *J Antibiot* 1991, **44**: 903-7.

Lam KS.
New aspects of natural products in drug discovery. *Trends Microbiol* 2007, **15**: 279-89.

Lim DS, Kwak YS, Kim JH, Ko SH, Yoon WH, Kim CH.
Antitumor efficacy of reticulol from Streptoverticillium against the lung metastasis

model B16F10 melanoma. Lung metastasis inhibition by growth inhibition of melanoma. *Chemotherapy* 2003, **49**: 146-53.

Lim DS, Kwak YS, Lee KH, Ko SH, Yoon WH, Lee WY, Kim CH.
Topoisomerase I inactivation by reticulol and its in vivo cytotoxicity against B16F10 melanoma. *Chemotherapy* 2003, **49**: 257-63.

Lum PY, Armour CD, Stepaniants SB, Cavet G, Wolf MK, Butler JS, Hinshaw JC, Garnier P, Prestwich GD, Leonardson A, Garrett-Engele P, Rush CM, Bard M, Schimmack G, Phillips JW, Roberts CJ, Shoemaker DD.
Discovering modes of action for therapeutic compounds using a genome-wide screen of yeast heterozygotes. *Cell* 2004, **116**: 121-37.

Nguyen T, Vinh DB, Crawford DK, Davis TN.
A genetic analysis of interactions with Spc110p reveals distinct functions of Spc97p and Spc98p, components of the yeast gamma-tubulin complex. *Mol Biol Cell* 1998, **9**: 2201-16.

Oki M, Noguchi E, Hayashi N, Nishimoto T.
Nuclear protein import, but not mRNA export, is defective in all *Saccharomyces cerevisiae* mutants that produce temperature-sensitive forms of the Ran GTPase homologue Gsp1p. *Mol Gen Genet* 1998, **257**: 624-34.

Overy DP, Larsen TO, Dalsgaard PW, Frydenvang K, Phipps R, Munro MH, Christophersen C.

Andrastin A and barceloneic acid metabolites, protein farnesyl transferase inhibitors from *Penicillium albocoremium*: chemotaxonomic significance and pathological implications. *Mycol Res* 2005, **109**: 1243-9.

Parsons AB, Geyer R, Hughes TR, Boone C.

Yeast genomics and proteomics in drug discovery and target validation. *Prog Cell Cycle Res* 2003, **5**: 159-66.

Schlenstedt G, Saavedra C, Loeb JD, Cole CN, Silver PA.

The GTP-bound form of the yeast Ran/TC4 homologue blocks nuclear protein import and appearance of poly(A)+ RNA in the cytoplasm. *Proc Natl Acad Sci USA* 1995, **92**: 225-9.

Sturgeon CM, Kemmer D, Anderson HJ, Roberge M.

Yeast as a tool to uncover the cellular targets of drugs. *Biotechnol J* 2006, **1**: 289-98.

Toussaint M, Conconi A.

High-throughput and sensitive assay to measure yeast cell growth: a bench protocol for testing genotoxic agents. *Nat Protoc* 2006, **1**: 1922-8.

Toussaint M, Levasseur G, Gervais-Bird J, Wellinger RJ, Elela SA, Conconi A.

A high-throughput method to measure the sensitivity of yeast cells to genotoxic agents in liquid cultures. *Mutat Res* 2006, **606**: 92-105.

Vertesy L, Aretz W, Ehlers E, Hawser S, Isert D, Knauf M, Kurz M, Schiell M, Vogel M, Wink J.

3874 H1 and H3, novel antifungal heptaene antibiotics produced by *Streptomyces* sp. HAG 003874. *J Antibiot* 1998, **51**: 921-8.

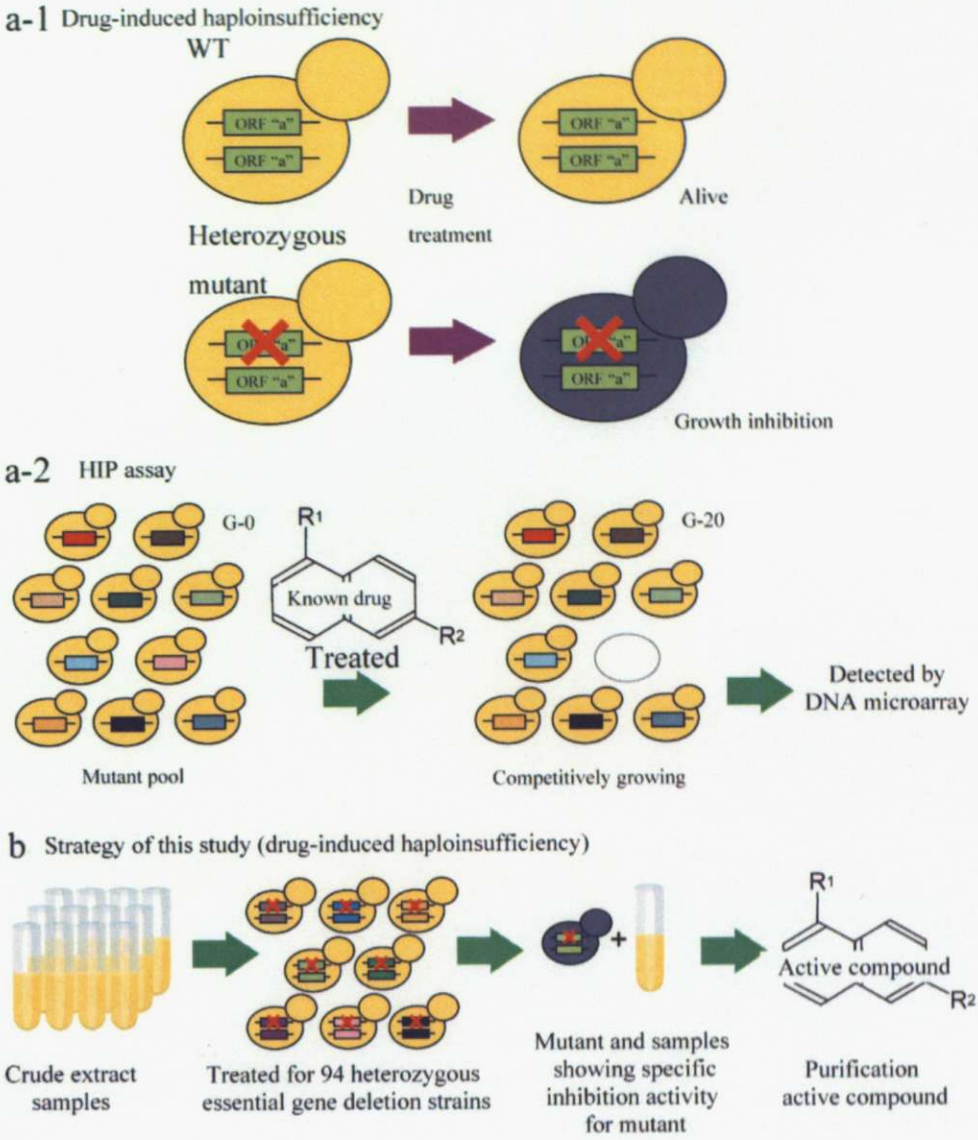

Figure 1 Premises for drug-induced haploinsufficiency screening

(a-1) A scheme of drug-induced haploinsufficiency
Reduction of target gene copy number can sensitize diploid cells to a drug.

(a-2) Conventional strategy using drug-induced haploinsufficiency; haploinsufficiency profiling assay (HIP assay)
HIP assay used to identify the known targets of a few well characterized compounds competitive growth experiments with small pools of heterozygous deletion mutants. Strain-specific molecular tags hybridized to DNA microarray were used to monitor the growth of individual heterozygous before and after drug treatment.

(b) The natural compound screening strategy of this study using drug-induced haploinsufficiency
To screen natural compounds and its target gene product, 94 heterozygous essential gene deletion strains were selected (94 mutants). 94 mutants were cultured in YPD medium or SD medium containing crude sample at 25 ° C for 28 hours. When there was a sample showing inhibition activity to a specific mutant, the sample was purified for active compound.

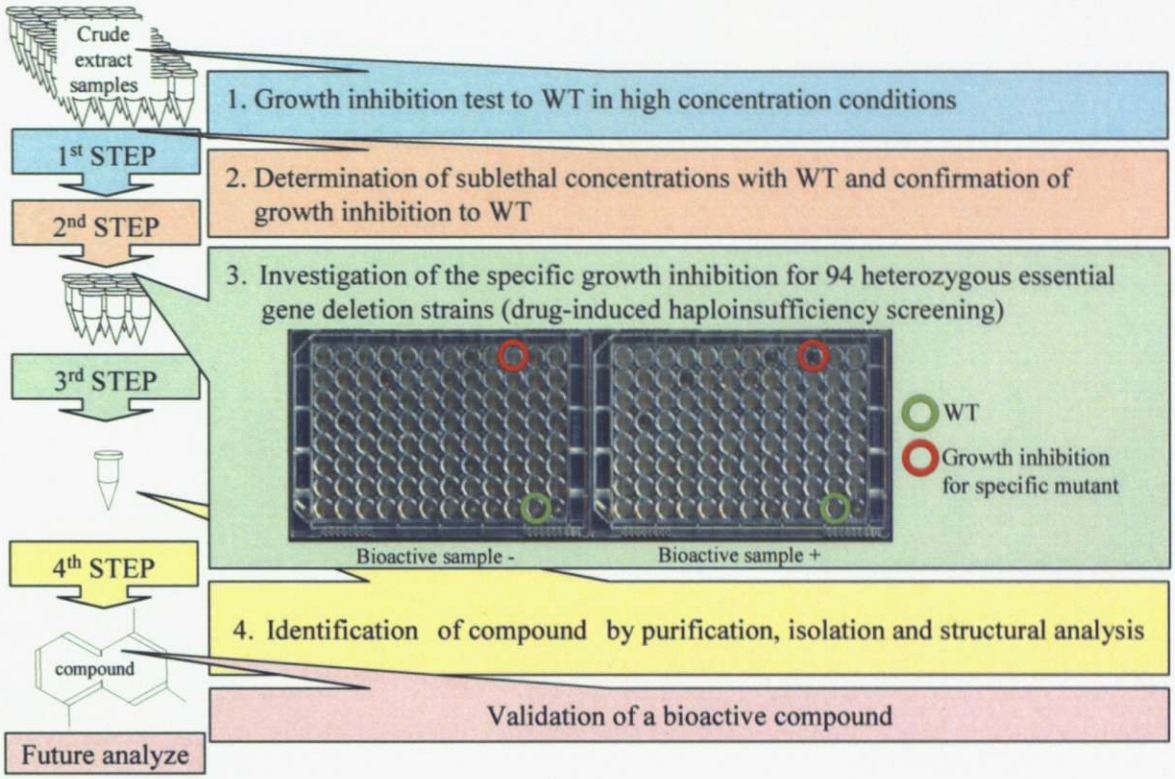

Figure 2 Strategy of screening

(1st STEP) To obtain a bioactive compound, screening strategy was established in composition of 4 steps. First, growth inhibition test to WT at a sample concentration of 5% (v/v) was examined.

(2nd STEP) Positive samples of minimum inhibitory concentrations (MIC) for WT were determined. In addition, reproducibility of 1st STEP was confirmed.

(3rd STEP) The specific growth inhibition in 94 heterozygous mutants investigated at each concentration which did not inhibit WT (half of MIC).

(4th STEP) To identify a compound from a sample that showed the specific growth inhibition to several mutants, purification, isolation and structural analysis were performed for the sample. Further validation analysis of an identified compound was performed.

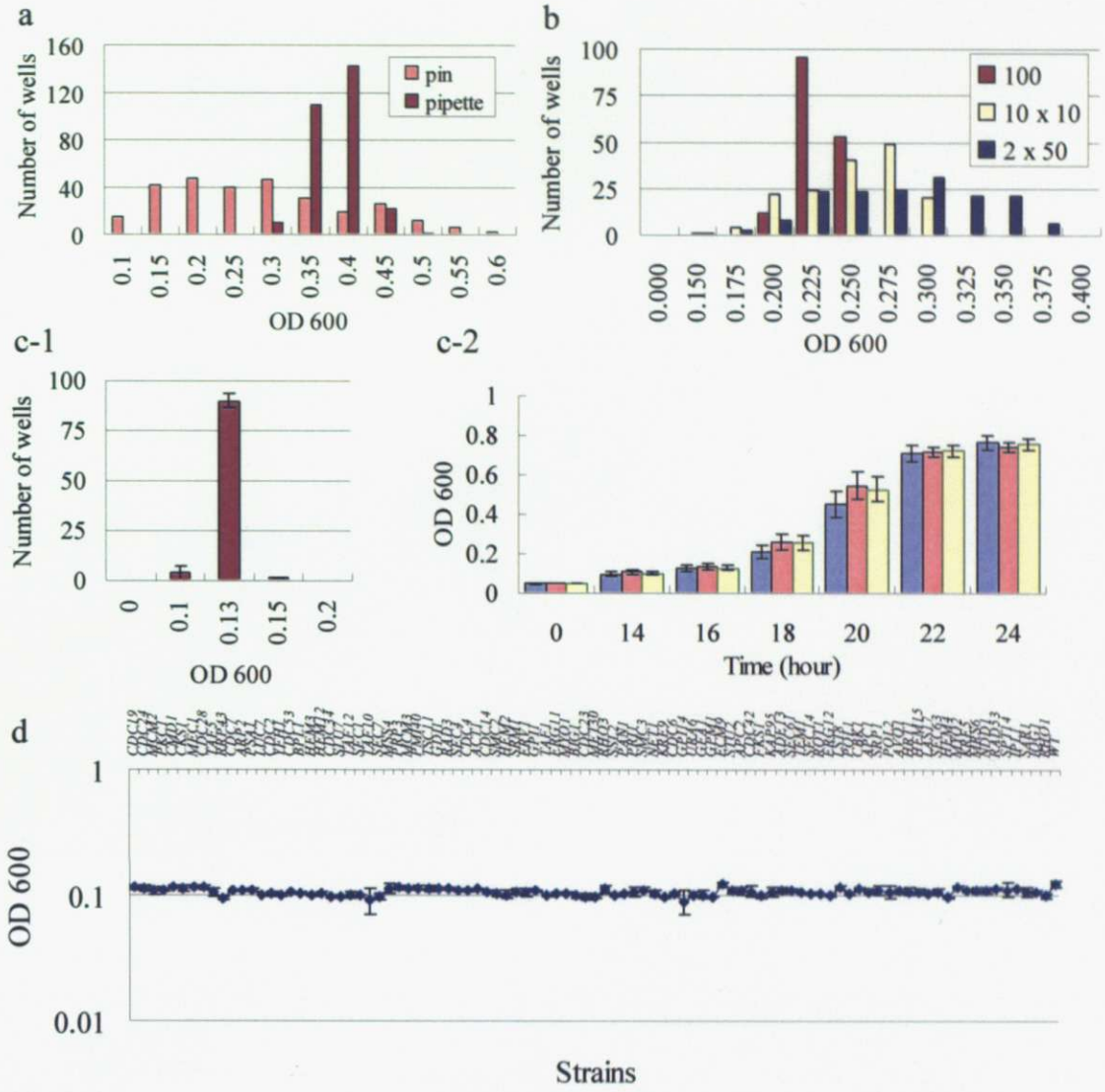

Figure 3 Examinations of inoculation and confirmation of culture condition
c and d were performed in triplicate and represent the average of three experiments.

(a) Examination of inoculation method from saturated culture medium to fresh liquid medium
The precision of two methods (pin method and pipette method) was compared using WT overnight culture. Cultures which inoculated by two methods were incubated at 25 °C for 6 hours, and OD 600 of culture was measured.

(b) Examination of the dilution method of the culture medium
WT overnight culture was diluted by three 100-fold dilution methods: 1) 100-fold by one-step (100), 2) 10-fold x 10-fold (10 x 10) and 3) 2-fold x 50-fold (2 x 50). 100 µl of diluted culture was dispensed to 96-well microplate and was cultured for 6 hours and its OD 600 was measured.

(c) Precision confirmation of screening system in 96-well microplate
WT overnight culture in 96-well microplate was diluted 100-fold on 96-deep plate, and 100 µl diluted culture were dispensed to 96-well microplate. Culture was incubated at 25 °C for 6 hours, and OD 600 was measured (c-1). Sequential transition of OD 600 was measured in WT culture (c-2).

(d) Distribution of OD 600 of 94 mutants with 96-well microplate
94 heterozygous essential gene deletion strains were cultured in actual screening condition and OD 600 of culture after 6 hour-incubation was measured.

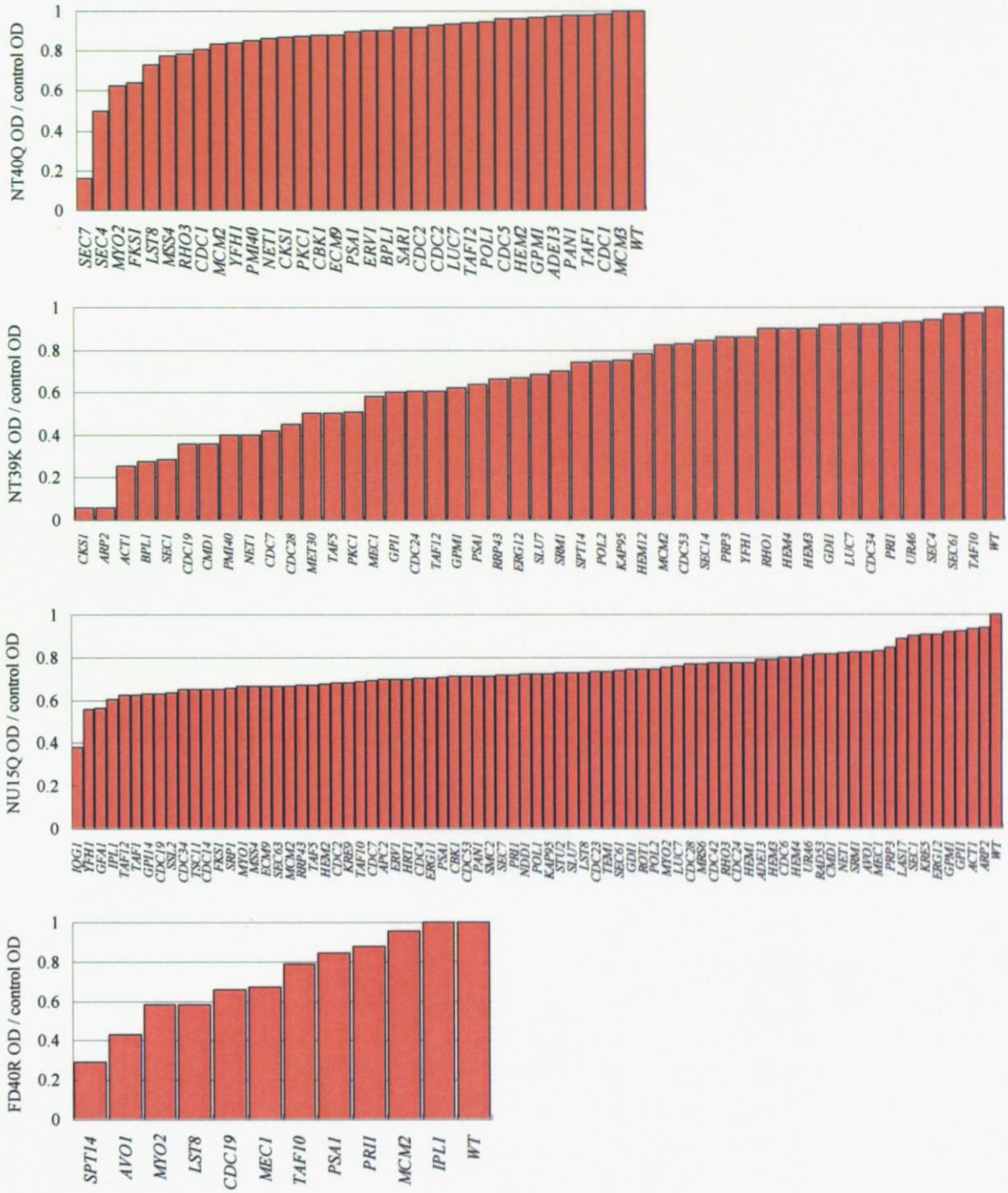

Figure 4 Samples which showed specific growth inhibition activity to mutants by drug-induced haploinsufficiency screening

The relative ratio (drug OD 600 / control OD 600) was calculated using the value of OD 600 which was measured after 22 hours from culture onset. The small relative ratio indicate that drug-induced haploinsufficiency was observed. Relative ratio was standardized using the value of WT. Strains of "the relative ratio < 1"were shown in graph.

neocarazostatin

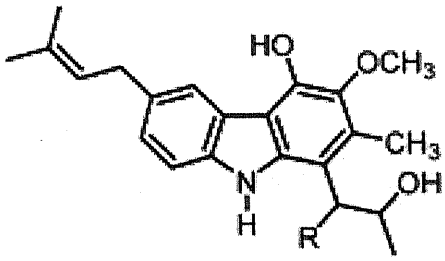

R = OH : neocarazostatin A
R = H : neocarazostatin B

tensidol B

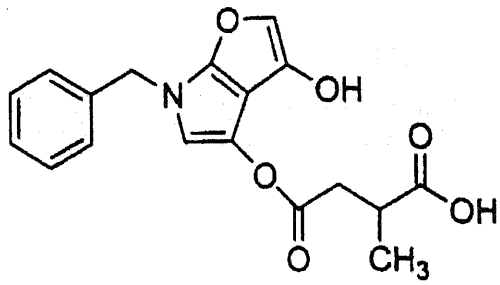

cycloheximide

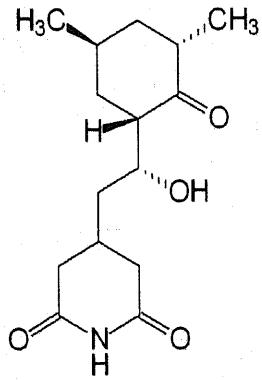

reticulol

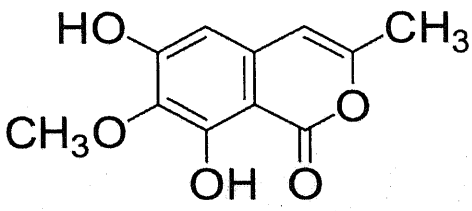

3874 H1

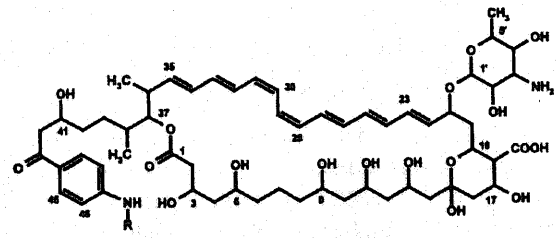

R = H

barceloneic acid B

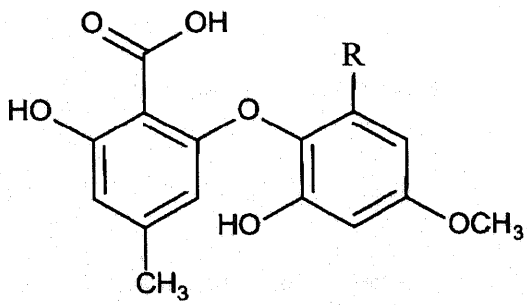

R = COOH : barceloneic acid B

Figure 5 Structure of identified compounds
References of the structures above are described in Discussion.

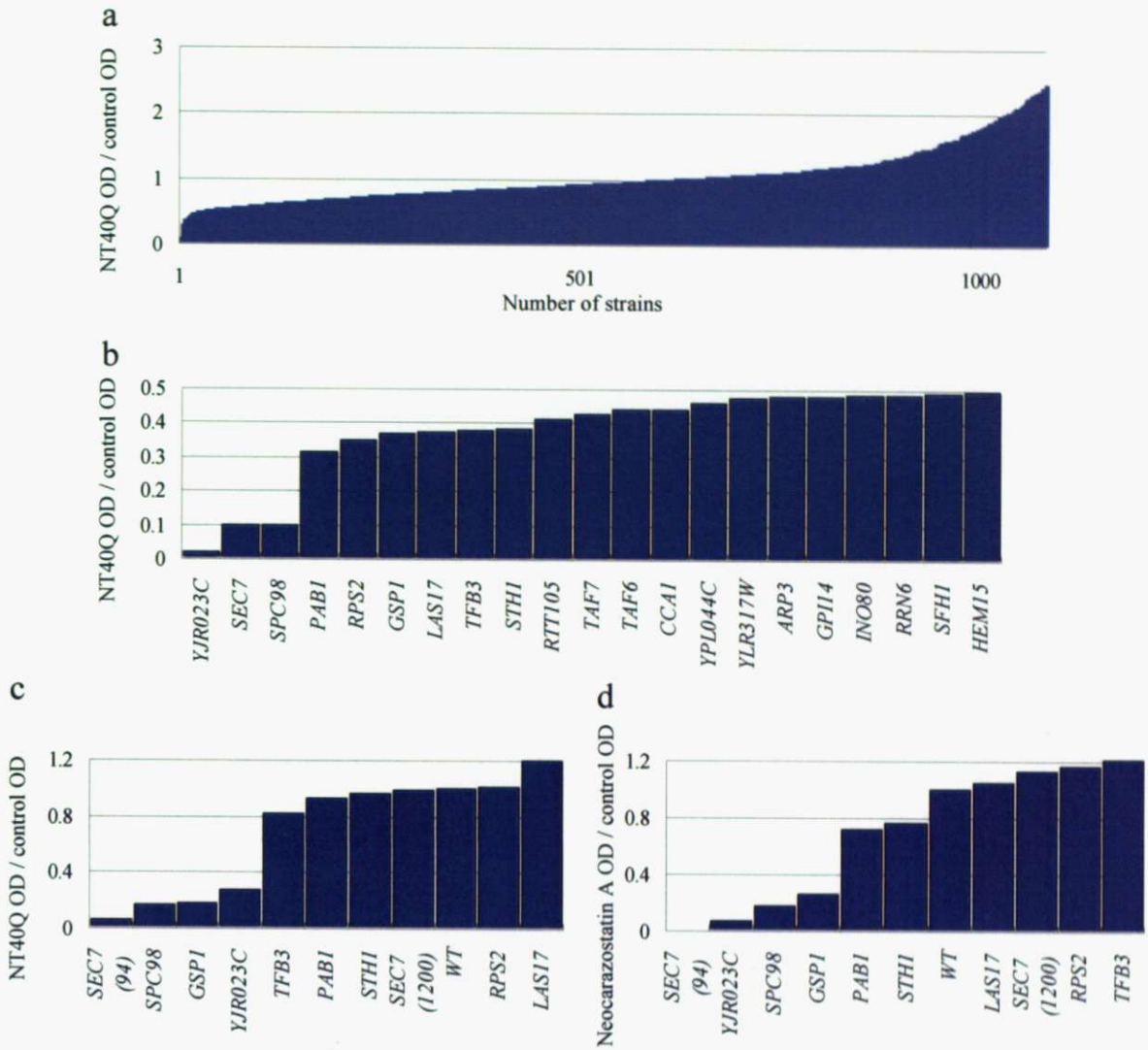

Figure 6 Confirmation of specific growth inhibition of NT40Q (neocarazostatin A) for all heterozygous essential gene deletion strains

The relative ratio (drug OD 600 / control OD 600) was calculated using the value of OD 600 which was measured after 22 hours from culture onset. The small relative ratio indicate that drug-induced haploinsufficiency was observed.

(a) Results of drug-induced haploinsufficiency assay for 1112 heterozygous essential gene deletion strains in 0.625% of NT40Q.

(b) Mutants showing remarkable growth inhibitory activity in (a).

(c) The reproducibility of growth inhibitory activity of NT40Q was confirmed to selected mutants. The relative ratio of the growth inhibitory activity was shown in a range of "drug OD 600 / control OD 600 < 0.4."

(d) Sensitive mutants for NT40Q were treated in 5 μg/ml neocarazostatin A (half of MIC).

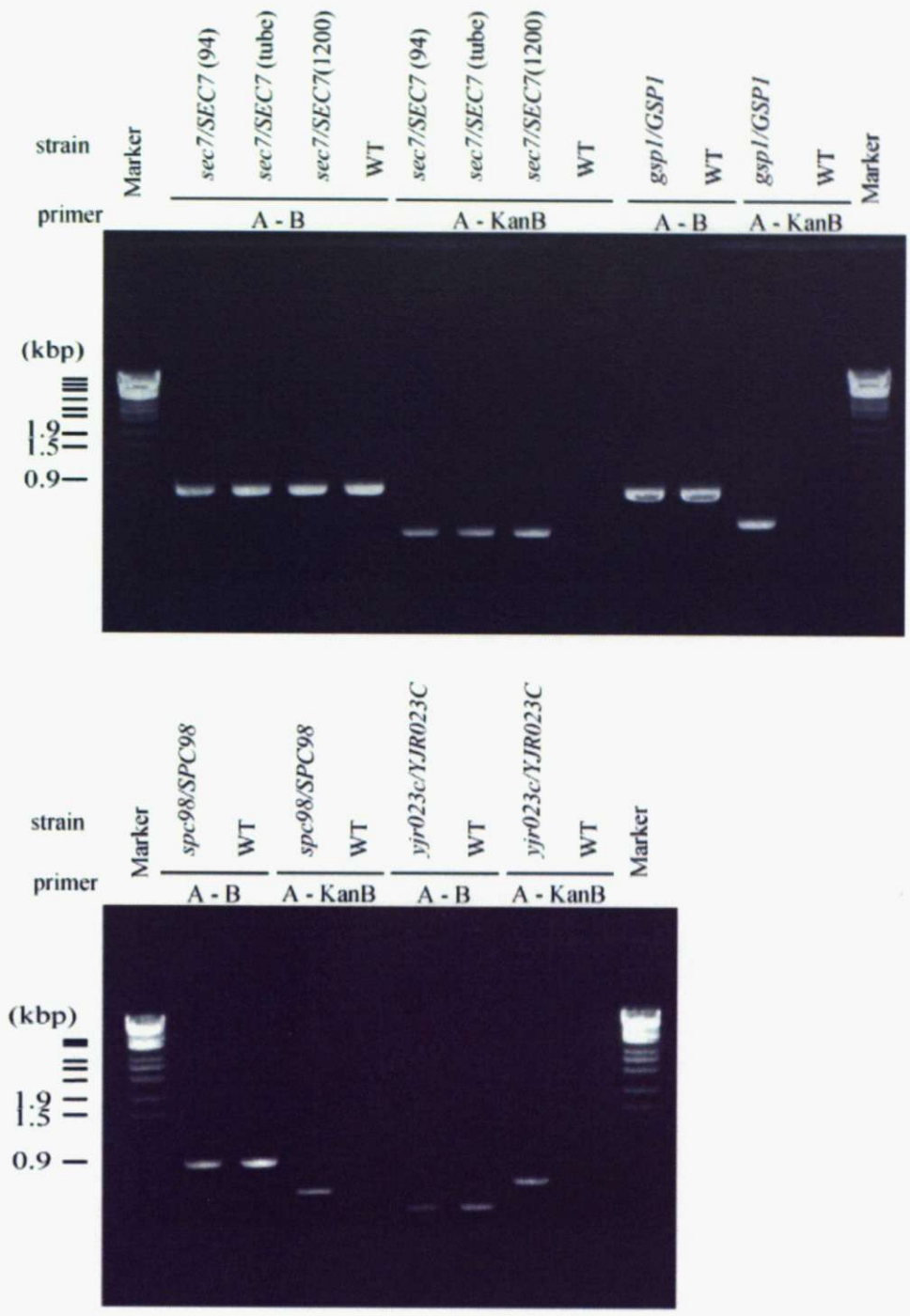

Figure 7 Strain confirmation of neocarazostatin A sensitive mutants
Disruption of the corresponding genes by replacement kanamycin-resistant gene cassette was confirmed by PCR. DNA which was extracted from cells cultured overnight at 25 °C and was amplified by PCR with using appropriate primers (Table 3). PCR product sizes were confirmed by agarose electrophoresis.

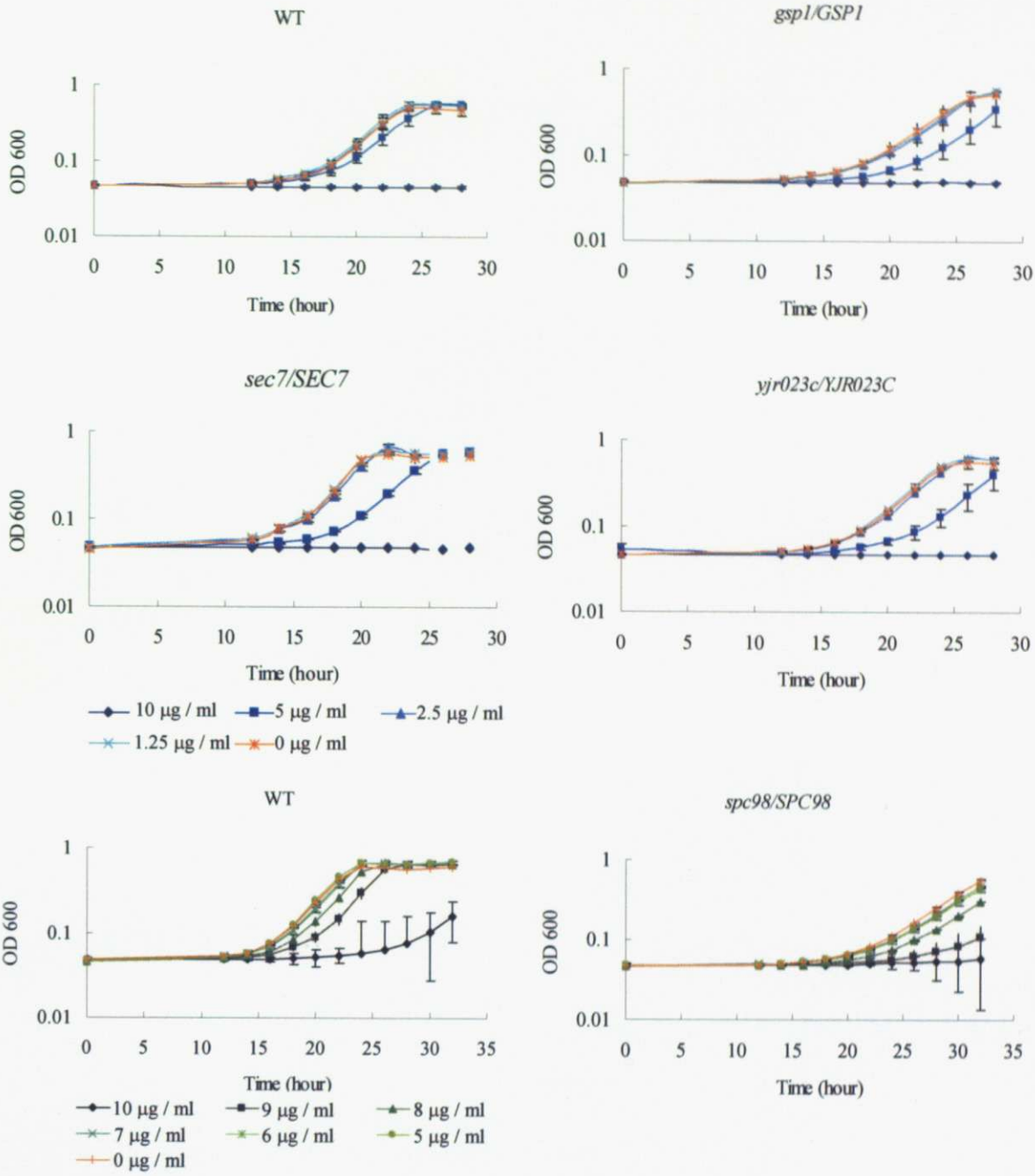

Figure 8 Neocarazostatin A sensitivity of its target candidates
Growth curves of mutants that cultured in YPD containing neocarazostatin A were described. Cells were incubated in the presence of various concentration of neocarazostatin A at 25 °C and OD 600 was measured every two hours from 14 hours to 24 hours.

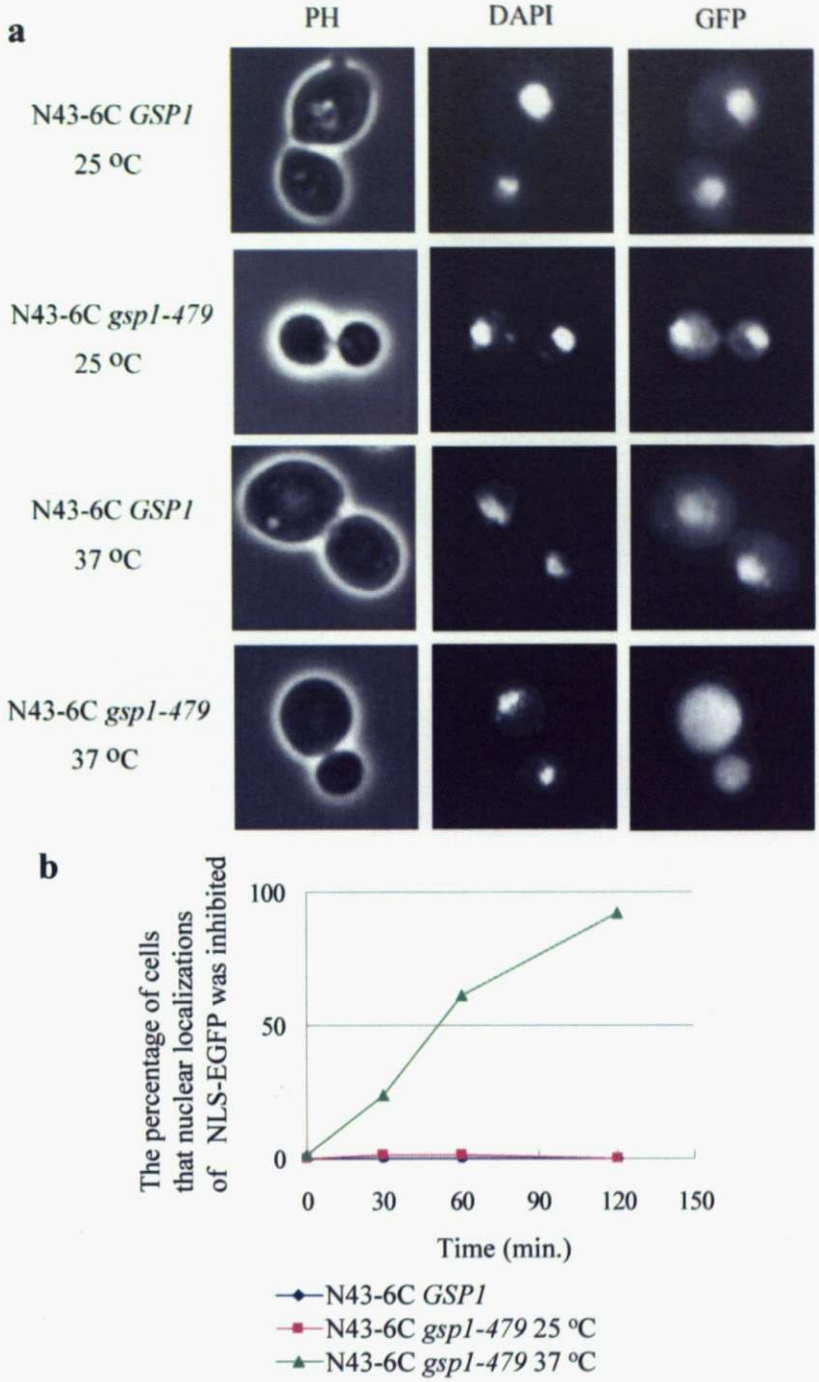

Figure 9 NLS-EGFP translocation requires the activity of Gsp1p
N43-6C *GSP1*, *gsp-479* strains were transformed with NLS-EGFP.

(a) Cells from overnight cultures were shifted up to nonpermissive temperature (37 °C) and incubated for 2 hour. NLS-EGFP was localized as described.

(b) The cells that nuclear localization of NLS-EGFP was inhibited were counted after 30, 60 and 120 minutes from cultures onset.

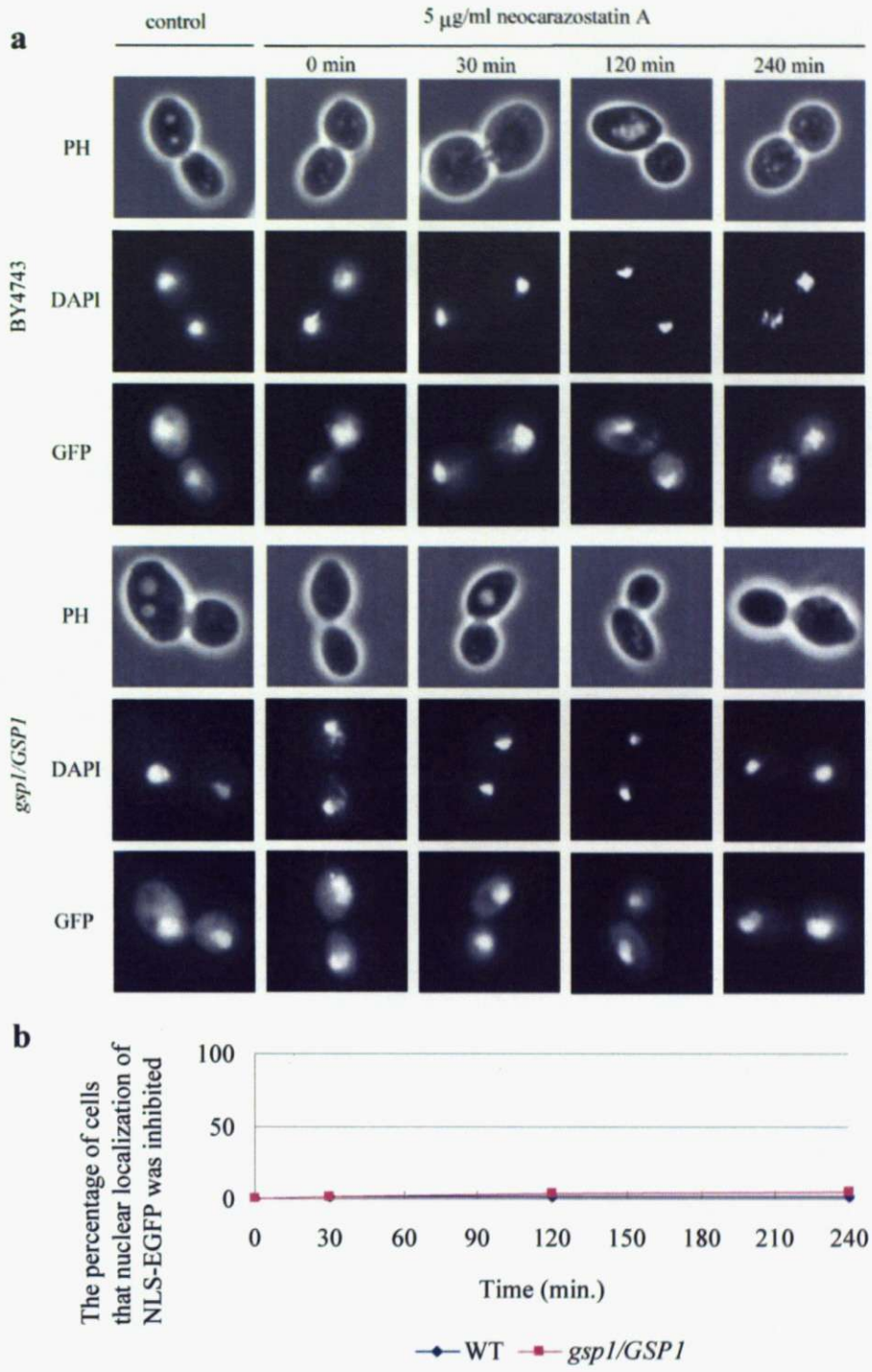

Figure 10 Neocarazostatin A does not inhibit nuclear localization of NLS-EGFP at 5 μg/ml (half of MIC)

(a) WT or *gsp1/GSP1* from logarithmic culture were incubated in the presence of 5 μg/ml neocarazostatin A at 25 °C for 4 hour. Cells were collected after 0, 30, 120, 240 minutes from cultures onset, and were observed nuclear localizations of NLS-EGFP.

(b) The cells that nuclear localization of NLS-EGFP was inhibited were counted by observation.

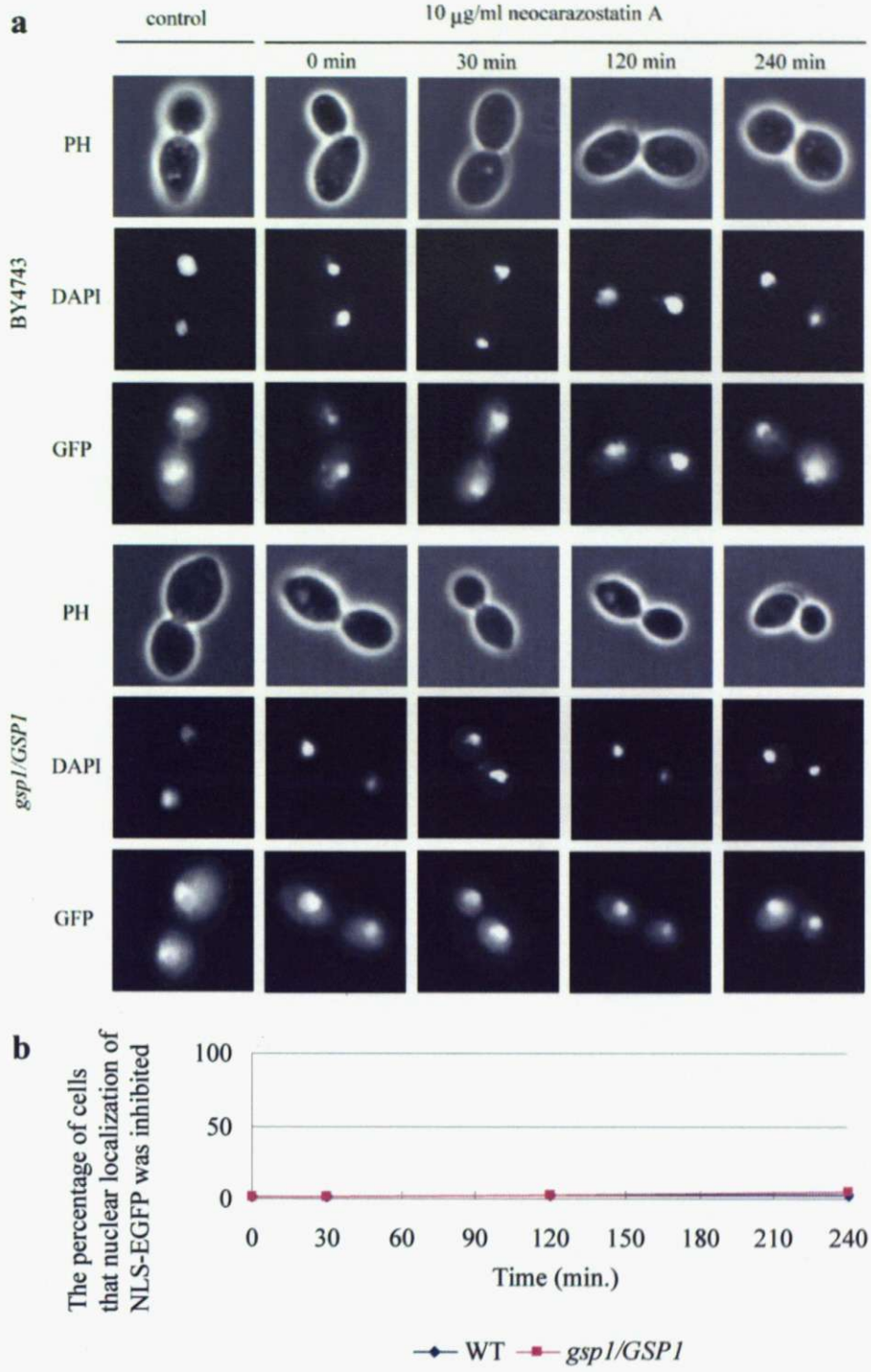

Figure 11 Neocarazostatin A does not inhibit nuclear localization of NLS-EGFP at 10 μg/ml (MIC)

(a) WT and *gsp1/GSP1* from logarithmic culture were incubated in the presence of 10 μg/ml neocarazostatin A at 25 °C for 4 hour. Cells were collected after 0, 30, 120, 240 minutes from cultures onset, and were observed nuclear localizations of NLS-EGFP.

(b) The cells that nuclear localization of NLS-EGFP was inhibited was counted by observation.

Table 1 Heterozygous deletion strains used in drug-induced haploinsufficiency screening in this study

Category	No.	ORF	Gene	Description
Human disease-associated genes	1	YAL038W	*CDC19*	Pyruvate kinase, functions as a homotetramer in glycolysis to convert phosphoenolpyruvate to pyruvate, the input for aerobic (TCA cycle) or anaerobic (glucose fermentation) respiration
	2	YBR136W	*MEC1*	Genome integrity checkpoint protein and PI kinase superfamily member; signal transducer required for cell cycle arrest and transcriptional responses prompted by damaged or unreplicated DNA; monitors and participates in meiotic recombination Huntington's disease, SCA2
	3	YCR035C	*RRP43*	Protein involved in rRNA processing; component of the exosome 3->5 exonuclease complex with Rrp41p, Rrp42p, Rrp4p and Dis3p; required for efficient maturation of 5.8S, 18S and 25S rRNA gonococcal disease
	4	YDL087C	*LUC7*	Essential protein associated with the U1 snRNP complex; splicing factor involved in recognition of 5' splice site alpha-thalassemia
	5	YDL120W	*YFH1*	Frataxin, regulates mitochondrial iron accumulation; interacts with Isu1p which promotes Fe-S cluster assembly; interacts with electron transport chain components and may influence respiration; human homolog involved in Friedrich's ataxia neurodegenerative disease
	6	YDL141W	*BPL1*	Biotin:apoprotein ligase, covalently modifies proteins with the addition of biotin, required for acetyl-CoA carboxylase (Acc1p) holoenzyme formation brain and mascle disease
	7	YDL205C	*HEM3*	Phorphobilinogen deaminase, catalyzes the conversion of 4-porphobilinogen to hydroxymethylbilane, the third step in the heme biosynthetic pathway; localizes to both the cytoplasm and nucleus; expression is regulated by Hap2p-Hap3p river disesase
	8	YDR047W	*HEM12*	Uroporphyrinogen decarboxylase, catalyzes the fifth step in the heme biosynthetic pathway; localizes to both the cytoplasm and nucleus; activity inhibited by Cu2+, Zn2+, Fe2+, Fe3+ and sulfhydryl-specific reagents heart,river,skindisease
	9	YDR088C	*SLU7*	RNA splicing factor, required for ATP-independent portion of 2nd catalytic step of spliceosomal RNA splicing; interacts with Prp18p; contains zinc knuckle domain Alport syndrome, Sly
	10	YDR473C	*PRP3*	Splicing factor, component of the U4/U6-U5 snRNP complex , Retinitis pigmentosa
	11	YEL032W	*MCM3*	Protein involved in DNA replication; component of the Mcm2-7 hexameric complex that binds chromatin as a part of the pre-replicative complex Polycystic kidney disease
	12	YER136W	*GDI1*	GDP dissociation inhibitor, regulates vesicle traffic in secretory pathways by regulating the dissociation of GDP from the Sec4/Ypt/rab family of GTP binding proteins
	13	YER171W	*RAD3*	5' to 3' DNA helicase, involved in nucleotide excision repair and transcription; subunit of RNA polymerase II transcription initiation factor TFIIH; subunit of Nucleotide Excision Repair Factor 3 (NEF3); homolog of human XPD protein cancer
	14	YFR028C	*CDC14*	Protein phosphatase required for mitotic exit; located in the nucleolus until liberated by the FEAR and Mitotic Exit Network in anaphase, enabling it to act on key substrates to effect a decrease in CDK/B-cyclin activity and mitotic exit Coden's syndrome
	15	YGL040C	*HEM2*	Delta-aminolevulinate dehydratase, a homo-octameric enzyme, catalyzes the conversion of delta-aminolevulinic acid to porphobilinogen, the second step in the heme biosynthetic pathway; localizes to both the cytoplasm and nucleus liver disesase
	16	YGL097W	*SRM1*	Nucleotide exchange factor for Gsp1p, localizes to the nucleus, required for nucleocytoplasmic trafficking of macromolecules; potentially phosphorylated by Cdc28p an eye disease
	17	YGR029W	*ERV1*	Flavin-linked sulfhydryl oxidase localized to the mitochondrial intermembrane space, has a role in the maturation of cytosolic iron-sulfur proteins; ortholog of human hepatopoietin (ALR) Polycystic kidney disease
	18	YHR007C	*ERG11*	Lanosterol 14-alpha-demethylase, catalyzes the C-14 demethylation of lanosterol to form 4,4"-dimethyl cholesta-8,14,24-triene-3-beta-ol in the ergosterol biosynthesis pathway; member of the cytochrome P450 family Brain disease
	19	YIL046W	*MET30*	F-box protein containing five copies of the WD40 motif, controls cell cycle function, sulfur metabolism, and methionine biosynthesis as part of the ubiquitin ligase complex; interacts with and regulates Met4p, localizes within the nucleus brain disease
	20	YIL143C	*SSL2*	Component of the holoenzyme form of RNA polymerase transcription factor TFIIH, has DNA-dependent ATPase/helicase activity and is required, with Rad3p, for unwinding promoter DNA; involved in DNA repair; homolog of human ERCC3 canser
	21	YKL024C	*URA6*	Uridylate kinase, catalyzes the seventh enzymatic step in the de novo biosynthesis of pyrimidines, converting uridine monophosphate (UMP) into uridine-5'-diphosphate (UDP) blood disease
	22	YKL152C	*GPM1*	Tetrameric phosphoglycerate mutase, mediates the conversion of 3-phosphoglycerate to 2-phosphoglycerate during glycolysis and the reverse reaction during gluconeogenesis muscle
	23	YLR359W	*ADE13*	Adenylosuccinate lyase, catalyzes two steps in the 'de novo' purine nucleotide biosynthetic pathway mental,brain disesase

Table 1 (*continued*)

Category	No.	ORF	Gene	Description
Human disease-associated genes	24	YMR079W	*SEC14*	Phosphatidylinositol/phosphatidylcholine transfer protein involved in coordinate regulation of PtdIns and PtdCho metabolism, products of which are regulators in Golgi to plasma membrane transport; functionally homologous to mammalian PITPs brain, muscle disease
	25	YMR208W	*ERG12*	Mevalonate kinase, acts in the biosynthesis of isoprenoids and sterols, including ergosterol, from mevalonate mental, brain disease
	26	YNL161W	*CBK1*	Serine/threonine protein kinase that regulates cell morphogenesis pathways; involved in cell wall biosynthesis, apical growth, proper mating projection morphology, bipolar bud site selection in diploid cells, and cell separation neurodegenerative disease
	27	YNL189W	*SRP1*	Karyopherin alpha homolog, forms a dimer with karyopherin beta Kap95p to mediate import of nuclear proteins, binds the nuclear localization signal of the substrate during import; may also play a role in regulation of protein degradation Russel-Silver syndrome
	28	YOR176W	*HEM15*	Ferrochelatase, a mitochondrial inner membrane protein, catalyzes the insertion of ferrous iron into protoporphyrin IX, the eighth and final step in the heme biosynthetic pathway; Yfh1p mediates the use of iron by Hem15p liver, skin blood disease
	29	YOR181W	*LAS17*	Actin assembly factor, activates the Arp2/3 protein complex that nucleates branched actin filaments; localizes with the Arp2/3 complex to actin patches; homolog of the human Wiskott-Aldrich syndrome protein (WASP) liver, skin blood disease
	30	YOR254C	*SEC63*	Essential subunit of Sec63 complex (Sec63p, Sec62p, Sec66p and Sec72p); with Sec61 complex, Kar2p/BiP and Lhs1p forms a channel competent for SRP-dependent and post-translational SRP-independent protein targeting and import into the ER Polycystic liver
	31	YOR278W	*HEM4*	Uroporphyrinogen III synthase, catalyzes the conversion of hydroxymethylbilane to uroporphyrinogen III, the fourth step in the heme biosynthetic pathway blood, skin disease
	32	YOR370C	*MRS6*	Rab escort protein, forms a complex with the Ras-like small GTPase Ypt1p that is required for the prenylation of Ypt1p by protein geranylgeranyltransferase type II (Bet2p-Bet4p) choroideremia
	33	YPL153C	*RAD53*	Protein kinase, required for cell-cycle arrest in response to DNA damage; activated by trans autophosphorylation when interacting with hyperphosphorylated Rad9p Li-Fraumeni syndrome
	34	YPL175W	*SPT14*	UDP-GlcNAc-binding and catalytic subunit of the enzyme that mediates the first step in glycosylphosphatidylinositol (GPI) biosynthesis, mutations cause defects in transcription and in biogenesis of cell wall proteins blood disease
	35	YPL209C	*IPL1*	Aurora kinase involved in regulating kinetochore-microtubule attachments, associates with Sli15p, which stimulates Ipl1p kinase activity and promotes its association with the mitotic spindle, potential Cdc28p substrate bone disease
	36	YPL218W	*SAR1*	GTPase, GTP-binding protein of the ARF family, component of COPII coat of vesicles; required for transport vesicle formation during ER to Golgi protein transport Anderson disiase
Possible to analysis in our laboratory	37	YAL041W	*CDC24*	Guanine nucleotide exchange factor (GEF or GDP-release factor) for Cdc42p; required for polarity establishment and maintenance, and mutants have morphological defects in bud formation
	38	YBR109C	*CMD1*	Calmodulin; Ca++ binding protein that regulates Ca++ independent processes (mitosis, bud growth, actin organization, endocytosis, etc.) and Ca++ dependent processes (stress-activated pathways), targets include Nuf1p, Myo2p and calcineurin
	39	YGR216C	*GPI1*	Membrane protein involved in the synthesis of N-acetylglucosaminyl phosphatidylinositol (GlcNAc-PI), the first intermediate in the synthesis of glycosylphosphatidylinositol (GPI) anchors; human and mouse GPI1p are functional homologs
	40	YHR023W	*MYO1*	Type II myosin heavy chain, required for wild-type cytokinesis and cell separation; localizes to the actomyosin ring; binds to myosin light chains Mlc1p and Mlc2p through its IQ1 and IQ2 motifs respectively
	41	YIL118W	*RHO3*	Non-essential small GTPase of the Rho/Rac subfamily of Ras-like proteins involved in the establishment of cell polarity; GTPase activity positively regulated by the GTPase activating
	42	YLR229C	*CDC42*	Small rho-like GTPase, essential for establishment and maintenance of cell polarity; mutants have defects in the organization of actin and septins
	43	YLR347C	*KAP95*	Karyopherin beta, forms a dimeric complex with Srp1p (Kap60p) that mediates nuclear import of cargo proteins via a nuclear localization signal (NLS), interacts with nucleoporins to guide transport across the nuclear pore complex
	44	YML064C	*TEM1*	GTP-binding protein of the ras superfamily involved in termination of M-phase; controls actomyosin and septin dynamics during cytokinesis
	45	YPL242C	*IQG1*	Essential protein required for determination of budding pattern, promotes localization of axial markers Bud4p and Cdc12p and functionally interacts with Sec3p, localizes to the contractile ring during anaphase, member of the IQGAP family
	46	YPR165W	*RHO1*	GTP-binding protein of the rho subfamily of Ras-like proteins, involved in establishment of cell polarity; regulates protein kinase C (Pkc1p) and the cell wall synthesizing enzyme 1,3-beta-glucan synthase (Fks1p and Gsc2p)

Table 1 (*continued*)

Category	No.	ORF	Gene	Description
DNA replication	47	YBL023C	*MCM2*	Protein involved in DNA replication; component of the Mcm2-7 hexameric complex that binds chromatin as a part of the pre-replicative complex
	48	YDL017W	*CDC7*	DDK (Dbf4-dependent kinase) catalytic subunit required for firing origins and replication fork progression in mitosis through phosphorylation of Mcm2-7p complexes and Cdc45p; kinase activity correlates with cyclical DBF4 expression
	49	YLR045C	*STU2*	Microtubule-associated protein (MAP) of the XMAP215/Dis1 family; regulates microtubule dynamics during spindle orientation and metaphase chromosome alignment; interacts with spindle pole body component Spc72p
Cell-cycle	50	YDL102W	*CDC2*	Catalytic subunit of DNA polymerase delta; required for chromosomal DNA replication during mitosis and meiosis, intragenic recombination, repair of double strand DNA breaks, and DNA replication during nucleotide excision repair (NER)
	51	YFR031C	*SMC2*	Component of the condensin complex, essential SMC chromosomal ATPase family member that forms a complex with Smc4p to form the active ATPase; Smc2p/Smc4p complex binds DNA, possibly in the cleft formed by the coiled-coil of the folded dimer
	52	YHR166C	*CDC23*	Subunit of the anaphase-promoting complex/cyclosome (APC/C), which is a ubiquitin-protein ligase required for degradation of anaphase inhibitors, including mitotic cyclins, during the metaphase/anaphase transition
	53	YJL074C	*SMC3*	Subunit of the multiprotein cohesin complex required for sister chromatid cohesion in mitotic cells; also required, with Rec8p, for cohesion and recombination during meiosis; phylogenetically conserved SMC chromosomal ATPase family member
	54	YJL194W	*CDC6*	Essential ATP-binding protein required for DNA replication, component of the pre-replicative complex (pre-RC) which requires ORC to associate with chromatin and is in turn required for Mcm2-7p DNA association; homologous to S. pombe Cdc18p
	55	YLR127C	*APC2*	Subunit of the Anaphase-Promoting Complex/Cyclosome (APC/C), which is a ubiquitin-protein ligase required for degradation of anaphase inhibitors, including mitotic cyclins, during the metaphase/anaphase transition; similar to cullin Cdc53p
	56	YNL172W	*APC1*	Largest subunit of the Anaphase-Promoting Complex/Cyclosome (APC/C), which is a ubiquitin-protein ligase required for degradation of anaphase inhibitors, including mitotic cyclins, during the metaphase/anaphase transition
Transport	57	YDR164C	*SEC1*	Sm-like protein involved in docking and fusion of exocytic vesicles through binding to assembled SNARE complexes at the membrane; localization to sites of secretion (bud neck and bud tip) is dependent on SNARE function
	58	YDR170C	*SEC7*	Guanine nucleotide exchange factor (GEF) for ADP ribosylation factors involved in proliferation of the Golgi, intra-Golgi transport and ER-to-Golgi transport; found in the cytoplasm and on Golgi-associated coated vesicles
	59	YFL005W	*SEC4*	Secretory vesicle-associated Rab GTPase essential for exocytosis; associates with the exocyst component Sec15p and may regulate polarized delivery of transport vesicles to the exocyst at the plasma membrane
	60	YLR378C	*SEC61*	Essential subunit of Sec61 complex (Sec61p, Sbh1p, and Sss1p); forms a channel for SRP-dependent protein import and retrograde transport of misfolded proteins out of the ER; with Sec63 complex allows SRP-independent protein import into ER
DNA / RNA polymerase	61	YDR167W	*TAF10*	Subunit (145 kDa) of TFIID and SAGA complexes, involved in RNA polymerase II transcription initiation and in chromatin modification
	62	YGR274C	*TAF1*	TFIID subunit (145 kDa), involved in RNA polymerase II transcription initiation, has histone acetyltransferase activity, involved in promoter binding and G1/S progression
	63	YIR008C	*PRI1*	Subunit of DNA primase, which is required for DNA synthesis and double-strand break repair
	64	YNL102W	*POL1*	Catalytic subunit of the DNA polymerase alpha-primase complex, required for the initiation of DNA replication during mitotic DNA synthesis and premeiotic DNA synthesis
	65	YNL262W	*POL2*	Catalytic subunit of DNA polymerase epsilon, one of the major chromosomal DNA replication polymerases characterized by processivity and proofreading exonuclease activity; also involved in DNA synthesis during DNA repair
Cell wall organization and biogenesis	66	YBL105C	*PKC1*	Protein serine/threonine kinase essential for cell wall remodeling during growth; localized to sites of polarized growth and the mother-daughter bud neck; homolog of the alpha, beta, and gamma isoforms of mammalian protein kinase C (PKC)
	67	YDL055C	*PSA1*	GDP-mannose pyrophosphorylase (mannose-1-phosphate guanyltransferase), synthesizes GDP-mannose from GTP and mannose-1-phosphate in cell wall biosynthesis; required for normal cell wall structure
	68	YER003C	*PMI40*	Mannose-6-phosphate isomerase, catalyzes the interconversion of fructose-6-P and mannose-6-P; required for early steps in protein mannosylation

Table 1 (*continued*)

Category	No.	ORF	Gene	Description
Cell wall organization and biogenesis	69	YER093C	*TSC11*	Subunit of TORC2 (Tor2p-Lst8p-Avo1-Avo2-Tsc11p-Bit61p), a membrane-associated complex that regulates actin cytoskeletal dynamics during polarized growth and cell wall integrity; involved in sphingolipid metabolism; contains a RasGEFN domain
	70	YHR101C	*BIG1*	Integral membrane protein of the endoplasmic reticulum, required for normal content of cell wall beta-1,6-glucan
	71	YJL174W	*KRE9*	Glycoprotein involved in cell wall beta-glucan assembly; null mutation leads to severe growth defects, aberrant multibudded morphology, and mating defects
	72	YJR013W	*GPI14*	Glycosylphosphatidylinositol-alpha 1,4 mannosyltransferase I, involved in GPI anchor biosynthesis, requires Pbn1p for function; homolog of mammalian PIG-M
	73	YKL104C	*GFA1*	Glutamine-fructose-6-phosphate amidotransferase, catalyzes the formation of glucosamine-6-P and glutamate from fructose-6-P and glutamine in the first step of chitin biosynthesis
	74	YKR004C	*ECM9*	Non-essential protein of unknown function
	75	YLR342W	*FKS1*	Catalytic subunit of 1,3-beta-D-glucan synthase, functionally redundant with alternate catalytic subunit Gsc2p; binds to regulatory subunit Rho1p; involved in cell wall synthesis and maintenance; localizes to sites of cell wall remodeling
	76	YMR200W	*ROT1*	Protein that may be involved in cell wall function; mutations in rot1 cause cell wall defects, suppress tor2 mutations, and are synthetically lethal with rot2 mutations
	77	YNL006W	*LST8*	Protein required for the transport of amino acid permease Gap1p from the Golgi to the cell surface; component of the TOR signaling pathway; associates with both Tor1p and Tor2p;
	78	YOL078W	*AVO1*	Component of a membrane-bound complex containing the Tor2p kinase and other proteins, which may have a role in regulation of cell growth
	79	YOR336W	*KRE5*	Protein required for beta-1,6 glucan biosynthesis; mutations result in aberrant morphology and severe growth defects
Others	80	YBR135W	*CKS1*	Subunit of the Cdc28 protein kinase, required for mitotic proteolysis, may also be involved in the proteolysis of the G1 cyclins
	81	YBR160W	*CDC28*	Catalytic subunit of the main cell cycle cyclin-dependent kinase (CDK); alternately associates with G1 cyclins (CLNs) and G2/M cyclins (CLBs) which direct the CDK to specific substrates
	82	YBR198C	*TAF5*	Subunit (90 kDa) of TFIID and SAGA complexes, involved in RNA polymerase II transcription initiation and in chromatin modification
	83	YDL029W	*ARP2*	Essential component of the Arp2/3 complex, which is a highly conserved actin nucleation center required for the motility and integrity of actin patches; involved in endocytosis and membrane
	84	YDL132W	*CDC53*	Cullin, structural protein of SCF complexes (which also contain Skp1p, Cdc34p, and an F-box protein) involved in ubiquitination; SCF promotes the G1-S transition by targeting G1 cyclins and the Cln-CDK inhibitor Sic1p for degradation
	85	YDR054C	*CDC34*	Ubiquitin-conjugating enzyme or E2; together with Skp1p, Rbx1p, Cdc53p, and an F-box protein, forms a ubiquitin-protein ligase called the SCF complex which regulates cell cycle progression by targeting key substrates for degradation
	86	YDR145W	*TAF12*	Subunit (61/68 kDa) of TFIID and SAGA complexes, involved in RNA polymerase II transcription initiation and in chromatin modification, similar to histone H2A
	87	YDR208W	*MSS4*	Phosphatidylinositol-4-phosphate 5-kinase, involved in actin cytoskeleton organization and cell morphogenesis; multicopy suppressor of stt4 mutation
	88	YFL009W	*CDC4*	F-box protein required for G1/S and G2/M transition, associates with Skp1p and Cdc53p to form a complex, SCFCdc4, which acts as ubiquitin-protein ligase directing ubiquitination of the phosphorylated CDK inhibitor Sic1p
	89	YFL039C	*ACT1*	Actin, structural protein involved in cell polarization, endocytosis, and other cytoskeletal functions
	90	YIR006C	*PAN1*	Part of actin cytoskeleton-regulatory complex Pan1p-Sla1p-End3p, associates with actin patches on the cell cortex; promotes protein-protein interactions essential for endocytosis; previously thought to be a subunit of poly(A) ribonuclease
	91	YJL076W	*NET1*	Core subunit of the RENT complex, which is a complex involved in nucleolar silencing and telophase exit; stimulates transcription by RNA polymerase I and regulates nucleolar structure
	92	YOL133W	*HRT1*	RING finger containing subunit of Skp1-Cullin-F-box ubiquitin protein ligases (SCF); required for Gic2p, Far1p, Sic1p and Cln2p degradation; may tether Cdc34p (a ubiquitin conjugating enzyme or E2) and Cdc53p (a cullin) subunits of SCF
	93	YOR326W	*MYO2*	One of two type V myosins, involved in polarized distribution of mitochondria; required for mitochondrion and vacuole inheritance and nuclear spindle orientation; moves multiple cargo; reversibly phosphorylated in vivo
	94	YOR372C	*NDD1*	Transcriptional activator essential for nuclear division; localized to the nucleus; essential component of the mechanism that activates the expression of a set of late-S-phase-specific genes

Table 2 List of yeast strains used to identify target of neocarazostatin A

Strain	Genotype	
BY4743	*MAT* **a** */MAT* α*; his3* Δ *1/his3* Δ *1; leu2* Δ *0/leu2* Δ *0; met15* Δ *0/MET15; LYS2/lvs2* Δ *0: ura3* Δ *0/ura3* Δ *0*	a
N43-6C *GSP1*	*MAT* **a** Δ *gsp1::HIS3::GSP1::LEU2 ade2 leu2 trp1 ura3*	b
N43-6C *gsp1-479*	*MAT* **a** Δ *gsp1::HIS3::gsp1ts::LEU2 ade2 leu2 trp1 ura3*	b

a: EUROSCARF

b: Gift from Dr. N. Hayashi.

Table 3 Oligonucleotides used in this study

Name	Sequences 5'-3'
HK/ KanB	CTGCAGCGAGGAGCCGTAAT
MW/SEC7 confirmation A	CAAAGTTGGGATTTACATCATTTCT
MW/SEC7 confirmation B	GATAGTGATATGTTCCTCGTATGGG
MW/GSP1 confirmation A	TGTCATTAACAATCTCCTATCCCTC
MW/GSP1 confirmation B	GGATATCTTCCTCGGGTATAGTGTT
MW/SPC98 confirmation A	GTATGACCTACGCTTCTTTGGTAAA
MW/SPC98 confirmation B	GCAACAAATTCTAATTGTGGGTTAC
MW/YJR023C confirmation A	ATTGCTAACATCGAACAAATCAAAG
MW/YJR023C confirmation B	AAATGAGCATGTAATATGGGAAAAA

Table 4 Progress of compounds screening

STEP	positive samples / assay samples
1	482/ 4960
2	280 / 482
3	15 / 280
4	7/15

Table 5 Samples that showed drug-induced haploinsufficiency

Sample name	List of deletion genes in mutants which showed drug-induced haploinsufficiency (relative ratio < 0.4)	The compound which was identified	MIC (%)	Medium
NU15Q	*IQG1*	Reticulol	2.500%	SD
NT40Q	*SEC7*	Neocarazostatin A Neocarazostatin B	2.500%	YPD
FD40R	*SPT14*	Tensidol B	0.625%	SD
NT39K	*CKS1*	Cycloheximide	0.313%	YPD
FB24R	*IPL1, CDC19, MYO2*	Barcelonic acid	2.500%	SD
NU14Q	*KRE9, CKS1, PKC1*	The mixture of polyene compounds (3784	0.039%	YPD
FB58R	*KAP95, NDD1, RHO3, CDC42, PRI1, PKC1*	Inactivity	5.000%	SD
FD77V	*CDC19*	Inactivity	5.000%	YPD
OO71K	*IQG1*	Inactivity	2.500%	SD
FD41V	*MEC1, CDC19, ARP2, BPL1*	Inactivity	2.500%	YPD
OO31Q	*SEC7*	Inactivity	2.500%	YPD
FE22V	*ECM9*	Pending state for mysterious activity	1.250%	SD
FC37V	*NET1, GPM1*	Pending state for mysterious activity	0.625%	SD
NY63Q	*FKS1, TAF5*	Pending state for weak activity	0.625%	SD
FC29V	*PRP3, IPL1, GDI1, ERV1, YFH1, SSL2*	Cancel purification	0.156%	SD

Table 6 Strains that showed drug-induced haploinsufficiency for neocarazostatin A

ORF	Gene	Description (from SGD)
YDR170C	*SEC7*	Guanine nucleotide exchange factor (GEF) for ADP ribosylation factors involved in proliferation of the Golgi, intra-Golgi transport and ER-to-Golgi transport; found in the cytoplasm and on Golgi-associated
YJR023C	*YJR023C*	Putative protein of unknown function; open reading frame overlaps LSM8/YJR022W encoding an essential snRNP protein required for RNA processing and splicing
YNL126W	*SPC98*	Component of the microtubule-nucleating Tub4p (gamma-tubulin) complex; interacts with Spc110p at the spindle pole body (SPB) inner plaque and with Spc72p at the SPB outer plaque
YLR293C	*GSP1*	GTP binding protein (mammalian Ranp homolog) involved in the maintenance of nuclear organization, RNA processing and transport; regulated by Prp20p, Rna1p, Yrb1p, Yrb2p, Yrp4p, Yrb30p, Cse1p and Kap95p; yeast Gsp2p homolog